

Accepted Manuscript

Discovery of 4-(((4-(5-chloro-2-(((1s,4s)-4-((2-methoxyethyl)amino)cyclohexyl)amino)pyridin-4-yl)thiazol-2-yl)amino)methyl)tetrahydro-2H-pyran-4-carbonitrile (JSH-150) as a novel highly selective and potent CDK9 kinase inhibitor

Beilei Wang, Jiaxin Wu, Yun Wu, Cheng Chen, Fengming Zou, Aoli Wang, Hong Wu, Zhenquan Hu, Zongru Jiang, Qingwang Liu, Wei Wang, Yicong Zhang, Feiyang Liu, Ming Zhao, Jie Hu, Tao Huang, Juan Ge, Li Wang, Tao Ren, Yuxin Wang, Jing Liu, Qingsong Liu



PII: S0223-5234(18)30797-9

DOI: [10.1016/j.ejmech.2018.09.025](https://doi.org/10.1016/j.ejmech.2018.09.025)

Reference: EJMECH 10736

To appear in: *European Journal of Medicinal Chemistry*

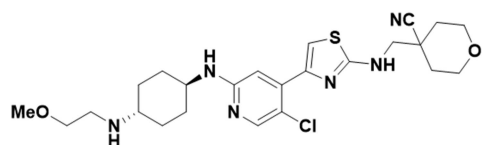
Received Date: 30 March 2018

Revised Date: 6 September 2018

Accepted Date: 9 September 2018

Please cite this article as: B. Wang, J. Wu, Y. Wu, C. Chen, F. Zou, A. Wang, H. Wu, Z. Hu, Z. Jiang, Q. Liu, W. Wang, Y. Zhang, F. Liu, M. Zhao, J. Hu, T. Huang, J. Ge, L. Wang, T. Ren, Y. Wang, J. Liu, Q. Liu, Discovery of 4-(((4-(5-chloro-2-(((1s,4s)-4-((2-methoxyethyl)amino)cyclohexyl)amino)pyridin-4-yl)thiazol-2-yl)amino)methyl)tetrahydro-2H-pyran-4-carbonitrile (JSH-150) as a novel highly selective and potent CDK9 kinase inhibitor, *European Journal of Medicinal Chemistry* (2018), doi: <https://doi.org/10.1016/j.ejmech.2018.09.025>.

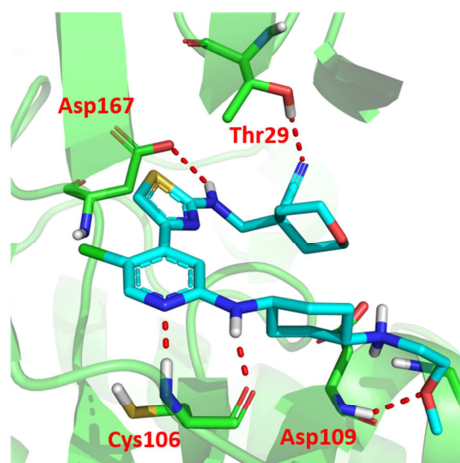
This is a PDF file of an unedited manuscript that has been accepted for publication. As a service to our customers we are providing this early version of the manuscript. The manuscript will undergo copyediting, typesetting, and review of the resulting proof before it is published in its final form. Please note that during the production process errors may be discovered which could affect the content, and all legal disclaimers that apply to the journal pertain.

**Compd. 40**CDK9 IC₅₀: 0.001 μMCDK7 IC₅₀: 1.72 μMp-RNA Pol II Ser2 EC₅₀: <0.1 μMMV4-11 GI₅₀: 0.012 μMMEC-1 GI₅₀: 0.037 μM

KINOMEScan S Score(1) = 0.01

T_{1/2} (mice): 1.55 h

F% (mice): 45%

Highly CDK9 selective

ACCEPTED MANUSCRIPT

Discovery **of**

4-(((4-(5-chloro-2-(((1s,4s)-4-((2-methoxyethyl)amino)cyclohexyl)amino)pyridin-4-yl)thiazol-2-yl)amino)methyl)tetrahydro-2H-pyran-4-carbonitrile (JSH-150) as a Novel Highly Selective and Potent CDK9 Kinase Inhibitor

Beilei Wang^{1,2,3,7}, *Jiaxin Wu*^{1,2,3,7}, *Yun Wu*^{1,3,7}, *Cheng Chen*^{1,2,3,7}, *Fengming Zou*^{1,3,7}, *Aoli Wang*^{1,3}, *Hong Wu*^{1,3}, *Zhenquan Hu*^{1,3}, *Zongru Jiang*^{1,2,3}, *Qingwang Liu*⁴, *Wei Wang*^{1,3}, *Yicong Zhang*^{1,2,3}, *Feiyang Liu*^{1,3}, *Ming Zhao*^{4,5}, *Jie Hu*^{4,5}, *Tao Huang*^{4,5}, *Juan Ge*^{4,5}, *Li Wang*^{1,2,3}, *Tao Ren*^{4,5}, *Yuxin Wang*⁵, *Jing Liu*^{1,3,4,5*}, *Qingsong Liu*^{1,2,3,4,5,6*}

1. High Magnetic Field Laboratory, Chinese Academy of Sciences, Mailbox 1110, 350 Shushanhu Road, Hefei, Anhui 230031, P. R. China
2. University of Science and Technology of China, Hefei, Anhui 230036, P. R. China
3. Key Laboratory of High Magnetic Field and Ion Beam Physical Biology, Hefei Institutes of Physical Science, Chinese Academy of Sciences, Hefei, Anhui 230031, P. R. China
4. Precision Targeted Therapy Discovery Center, Institute of Technology Innovation, Hefei Institutes of Physical Science, Chinese Academy of Sciences, Hefei, Anhui 230088, P. R. China
5. Precision Medicine Research Laboratory of Anhui Province, Hefei, Anhui 230088, P. R. China
6. Institute of Physical Science and Information Technology, Anhui University, Hefei, Anhui 230601, P. R. China

7. These authors contribute equally

AUTHOR INFORMATION

Corresponding Authors

*E-mail address: jingliu@hmfl.ac.cn (J.Liu), E-mail address: qslu97@hmfl.ac.cn (Q. Liu).

ABSTRACT

Through a structure-guided rational drug design approach, we have discovered a highly selective inhibitor compound **40** (JSH-150), which exhibited an IC_{50} of 1 nM against CDK9 kinase in the biochemical assay and achieved around 300-10000-fold selectivity over other CDK kinase family members. In addition, it also displayed high selectivity over other 468 kinases/mutants (KINOMEScan S score(1)=0.01). Compound **40** displayed potent antiproliferative effects against melanoma, neuroblastoma, hepatoma, colon cancer, lung cancer as well as leukemia cell lines. It could dose-dependently inhibit the phosphorylation of RNA Pol II, suppress the expression of MCL-1 and C-Myc, arrest the cell cycle and induce the apoptosis in the leukemia cells. In the MV4-11 cell-inoculated xenograft mouse model, 10 mg/kg dosage of **40** could almost completely suppress the tumor progression. The high selectivity and good in vivo PK/PD profile suggested that **40** would be a good pharmacological tool to study CDK9-mediated physiology and pathology as well as a potential drug candidate for leukemia and other cancers.

Keywords

CDK9, Kinase inhibitor, Structure-activity relationship, Leukemia

Abbreviations used

AML, acute myeloid leukemia; CDK, cyclin-dependent kinase; CLL, chronic lymphocytic leukemia; MCL, mantle cell lymphoma; SAR, structure-activity relationship; DMSO, dimethyl sulfoxide; DMF, N, N-dimethylformamide; DCM, dimethyl chloride; NBS, N-bromobutanamide; DMAP, 4-dimethylaminopyridine; LDA, lithium diisopropylamide; DIPEA, N, N-diisopropylethylamine; DME, 1,2-dimethoxyethane; DIAD, diisopropyl azodicarboxylate.

1. Introduction

Cyclin-dependent kinases (CDKs) are a class of serine/threonine protein kinase which play critical roles in the regulation of cell cycle or/and transcription [1,2]. To date, 21 different CDKs (1–11a, 11b–20) have been identified in the human genome and they can be divided into two main groups based on their primary roles [3]. CDK1, CDK2, CDK4, and CDK6 have been found to regulate the cell cycle progression upon binding to cyclin proteins. CDK7, CDK8, CDK9 and CDK11 are key players in transcription regulation [4,5]. These CDKs promote RNA synthesis for cell growth, differentiation and viral pathogenesis [6,7] etc. Among them, CDK9 is a key regulator of transcription elongation in eukaryotic cells and has been considered as a potential drug target for several diseases including cardiac hypertrophy and certain cancers such as a variety of blood cancers as well as solid tumors [8]. CDK9 phosphorylates Ser2 residues in the carboxy-terminal domain (CTD) of RNA Pol II to initiate the transcription elongation [9]. Activation of CDK9 kinase will promote the expression of antiapoptotic factor myeloid cell leukemia 1 (MCL-1) [10], which leads to malignant cell transformation. Inhibition of CDK9 activity will result in the down-regulation of this short-lived antiapoptotic protein MCL-1, and

consequently the induction of caspase-dependent apoptosis which is important for tumor control [11-14].

Flavopiridol (alvocidib, **1**), the first CDK inhibitor entered into clinical trials, exhibited antileukemic activity in CLL patients via potent inhibition of the CDK9-mediated down-regulation of antiapoptotic proteins transcription [15,16]. This has stimulated broad research interests for CDK9 and a number of small molecule inhibitors have been discovered and moved into clinical investigation (Figure 1). However, the high structural homology of ATP binding pocket among CDKs made it a great challenge for developing highly selective CDK9 kinase inhibitors. Most of the currently known CDK9 inhibitors are non-selective inhibitors. For example, **1** exhibited high potency against CDK1, 2, 4, 5, 6 and 9; **2** (SNS-032) was potent to CDK 2, 7 and 9 [17,18]; compound **3** (RGB286638) targeted CDK1, 2, 3, 4, 5 and 9. Compound **4** (LY2857785), which was evaluated in phase I clinical trials for the treatment of solid tumors, was relatively more selective but also simultaneously inhibited CDK7, 8, 9 [19,20]. Other multiple CDK inhibitors including **5** [21] (AZD5438, CDK1/2/9), **6** [22] (AT7519, CDK1/2/4/6/9) and **7** [23-25] (SCH727965, CDK1/2/5/9) have also been tested in clinical trials. The pyrimidine core scaffold-based CDK9 inhibitors including **8** (CDKI-73) [13] and **9** also potently inhibited both CDK7 and CDK9. However, given the fact that most of the CDK family members play critical roles both in physiology and pathology conditions, *e.g.*, CDK7 is directly upstream of CDK9 and both of them control transcription, non-specific inhibition of these kinases would increase the potential of the adverse events in the clinic and also made it hard to dissect the specific roles in the cellular context. Therefore, a highly selective CDK9 inhibitor is urgently desired for both of the physiological and

pathological study. Here we reported our medicinal chemistry efforts starting from **9**'s core scaffold which led to the discovery of a highly selective and potent CDK9 inhibitor **40** (JSH-150). It is worth mentioning that during preparation of this manuscript, a structurally similar inhibitor **10** (NVP-2), which also exhibited high selectivity and potency against CDK9 kinase, was reported as a chemical biology research tool for studying protein degradation [26].

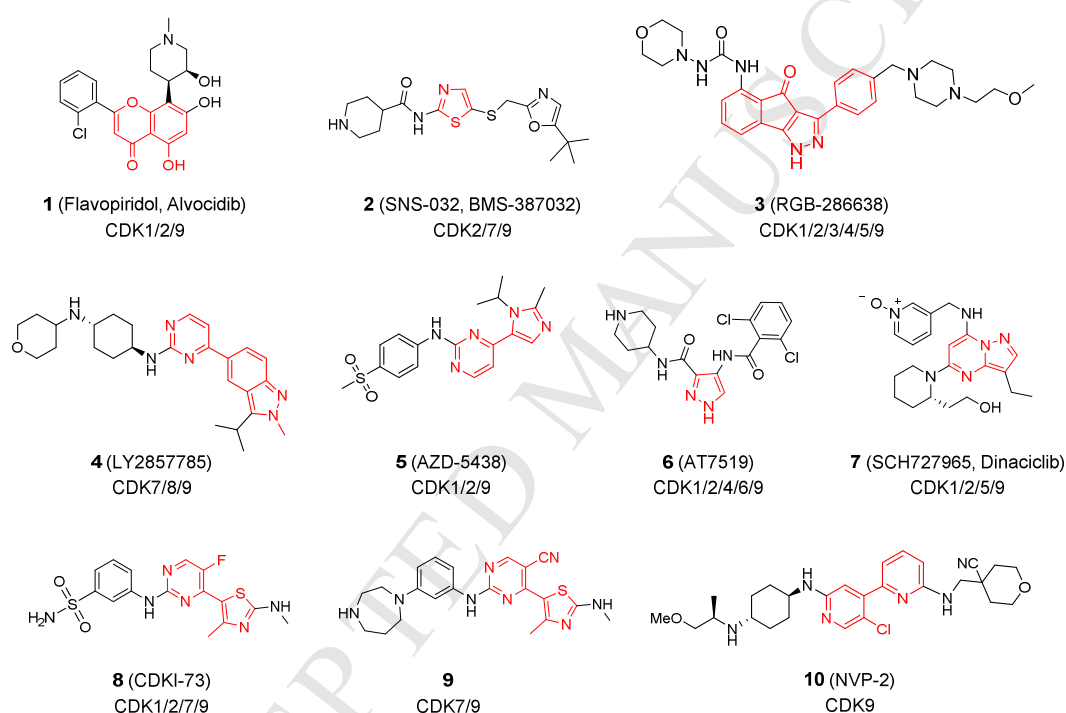


Figure 1. Chemical structures of representative inhibitors that bear CDK9 kinase activity.

2. Results and discussion

2.1. Design rationale

Compound **9** is a potent inhibitor of CDK9 with an IC_{50} of 14 nM, but also displays an IC_{50} value of 92 nM for CDK7 [27]. In order to compare the binding modes of **9** in CDK7 and CDK9, we docked **9** into the CDK7 kinase (PDB ID: 1UA2) [7] (Figure

2A-B). The results showed that the aminopyrimidine formed two hydrogen bonds in the hinge binding area with Met94 and Cys106 of CDK7 and CDK9 respectively. The diazepane moiety of **9** formed a hydrogen bond with Leu143 and Thr29 of CDK7 and CDK9 respectively. In addition, the NH of amino-thiazole moiety of **9** formed hydrogen bonds with Lys41 and Thr29 of CDK7 and CDK9 respectively. After carefully analyzing the structures of CDK7 and CDK9, we postulated that the P-loop of CDK9 was more flexible and could accommodate bigger fragments at this position than CDK7. In addition, there is a shallow hydrophobic pocket adjacent to the hinge binding area formed by His108 and Gly112 of CDK9. While for CDK7, these two residues were replaced by Thr96 and Val100, which indicated that a carefully selected small hydrophobic moiety could be used here to explore the selectivity between CDK7 and CDK9 (Figure 2C-D). Furthermore, the structural information showed that the gatekeeper residue in both CDK7 (Phe91) and CDK9 (Phe103) interacted with the CN group of **9**, which might be replaced with the Cl atom in order to achieve higher binding affinity due to the halogen bond interaction [28]. Based on these analyses, we decided to start from **9**'s core scaffold and modify the R¹/R²/R³, X and Y moieties, which finally led to the discovery of the highly potent and selective CDK9 kinase inhibitor **40** (JSH-150) (Figure 3).

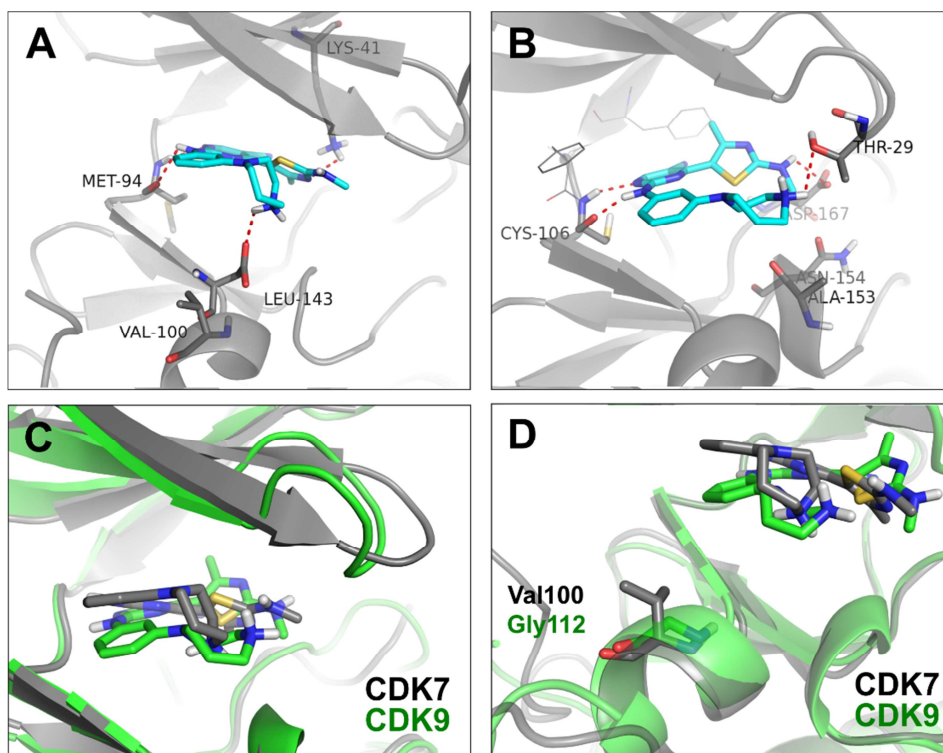


Figure 2. Binding mode of compound **9** with CDK7/9 kinase. (A) Docking of **9** in CDK7 kinase (PDB ID: 1UA2). (B) X-ray structure of **9** in complex with CDK9 kinase (PDB ID: 4BCG). (C) Illustration of the P-loop area difference by overlaying CDK7 and CDK9. (D) Illustration of the sequence difference of CDK7 and CDK9 adjacent to the hinge binding area.

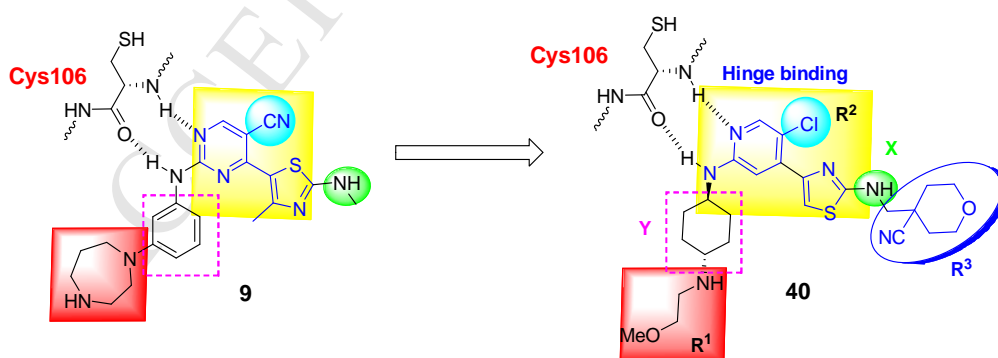
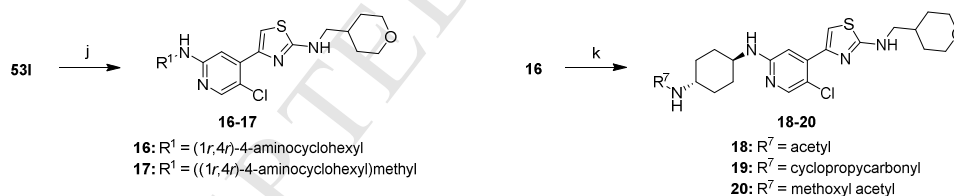
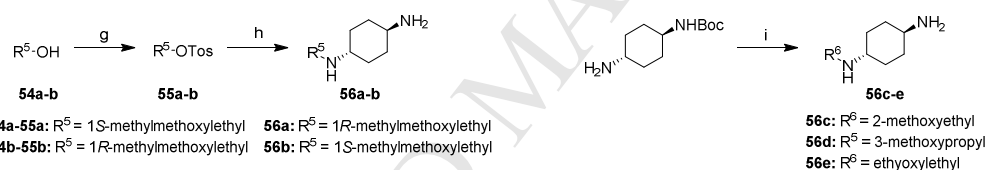
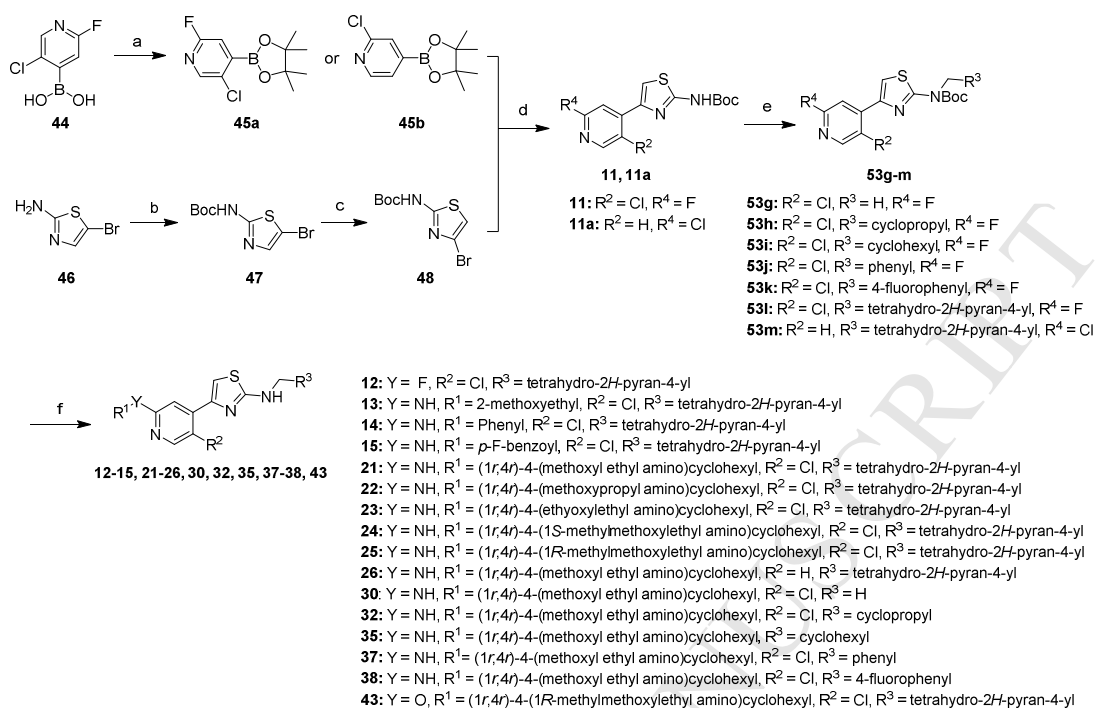


Figure 3. Schematic illustration of discovery of compound **40** from compound **9**.

2.2. Chemistry and structure-activity relationship (SAR) investigation

As shown in scheme 1, 5-bromothiazol-2-amine (**46**) was protected with Boc group (**47**) and intermediate **48** was prepared via Bromine dance reaction. Suzuki coupling between **48** and pinacol boronic ester **45a** or **45b** offered intermediates **11** or **11a**, which then reacted with appropriate alcohols to afford intermediates **53g-m** via Mitsunobu reaction. Intermediates **56a-b** were prepared from corresponding alcohols (**54a-b**) via tosylation reaction (**55a-b**) and nucleophilic substitution, while **56c-e** were synthesized from *tert*-butyl ((1*r*,4*r*)-4-aminocyclohexyl)carbamate after nucleophilic substitution with alkyl bromide and Boc deprotection. The target compounds **12-15**, **21-26**, **30**, **32**, **35**, **37-38** and **43** were obtained by nucleophilic substitution of **53g-m** with **56a-e**. Nucleophilic substitution of **53i** with appropriate Boc-protected amine followed by deprotection of the Boc group furnished the target compounds **16-17**, and **18-20** were obtained by acylation reaction of **16** with corresponding acyl chloride (Scheme 1).

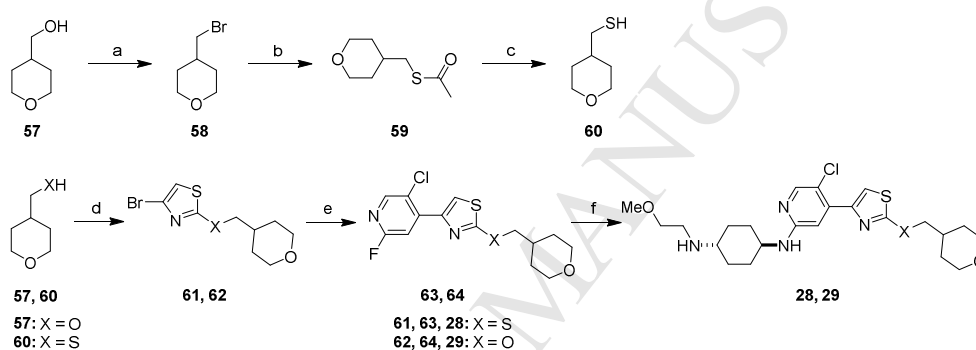
Scheme 1. Synthesis of Compounds **11-26**, **30**, **32**, **35**, **37-38** and **43**^a



^aReagents and conditions: (a) pinacol, toluene, reflux, overnight; (b) Boc₂O, DMAP, THF, rt, 2 days; (c) LDA, 0 °C, 2 h; (d) Pd(PPh₃)₄, Na₂CO₃, DME/H₂O/dioxane, 70 °C, overnight; (e) R³CH₂OH, PPh₃, DIAD, THF, N₂, 0 °C, overnight; (f) R¹NH₂ or R¹OH, DIEA, DMSO, 100-110 °C, 2 days; (g) NaH, TosCl, 0 °C-rt, overnight; (h) trans-1,4-diaminocyclohexane, CH₃CN, 90 °C, overnight; (i) (i) R⁶-Br, K₂CO₃, CH₃CN, 80 °C, 16 h; (ii) 4 N HCl, ethyl acetate, rt, 3 h; (j) (i) R¹NHBoc, DIEA, DMSO, 100-110 °C, 2 days; (ii) CF₃COOH, DCM, 0 °C-rt, 1.5 h; (k) R⁷COCl, DCM, 0 °C, 1 h.

The syntheses of compounds **28-29** were depicted in Scheme 2. Intermediate **60** was synthesized from (tetrahydro-2*H*-pyran-4-yl)methanol (**57**) in three steps including bromination (**58**), nucleophilic substitution (**59**) and reduction. Then a nucleophilic substitution reaction between **57/60** with 2, 4-dibromothiazole provided intermediates **61-62**. Suzuki coupling between **61/62** and **45a** afforded **63-64**, which was subsequently subjected to nucleophilic substitution with **56c** to yield the target compounds **28-29**.

Scheme 2. Synthesis of Compounds **28-29**^a

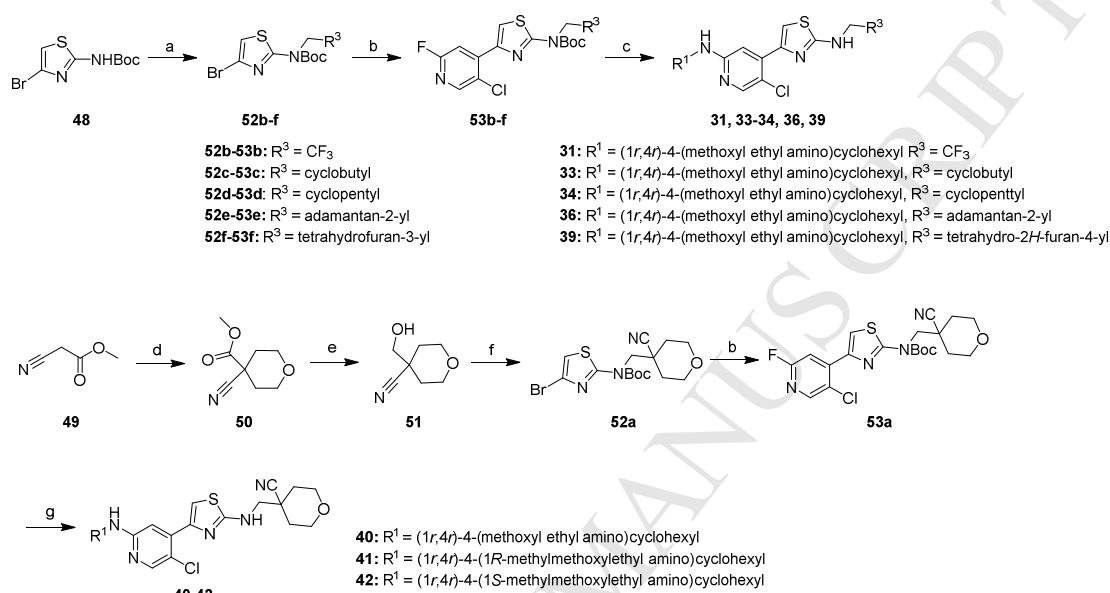


^aReagents and conditions: (a) NBS, PPh₃, DCM, 0 °C, 1-2 h; (b) KSAc, DMF, 90 °C, 2 h; (c) LiAlH₄, THF, 0 °C-rt, overnight; (d) 2,4-dibromothiazole, NaH, THF, 0 °C-rt, overnight; (e) **45a**, Pd(PPh₃)₄, Na₂CO₃, 1,4-dioxane/H₂O, 90 °C, overnight; (f) **56c**, K₂CO₃, DMSO, 100 °C, 2 days.

Starting from Mitsunobu reaction between **48** and a variety of alcohols, which afforded intermediates **52b-f**, compounds **31**, **33-34**, **36** and **39** were obtained from nucleophilic substitution of **56c** and **53b-f** which were provided by Suzuki coupling between **52b-f** and **45a**. For the syntheses of **40-42**, intermediate **51** was obtained through a two-step process including cyclization (**50**) and reduction. Then Mitsunobu reaction between **51** and **48** offered intermediate **52a**, which was subjected to a Suzuki coupling

with **45a** to yield **53a**. Finally, a base-mediated substitution reaction between **56a-c** and **53a** furnished the desired compounds **40-42** (Scheme 3).

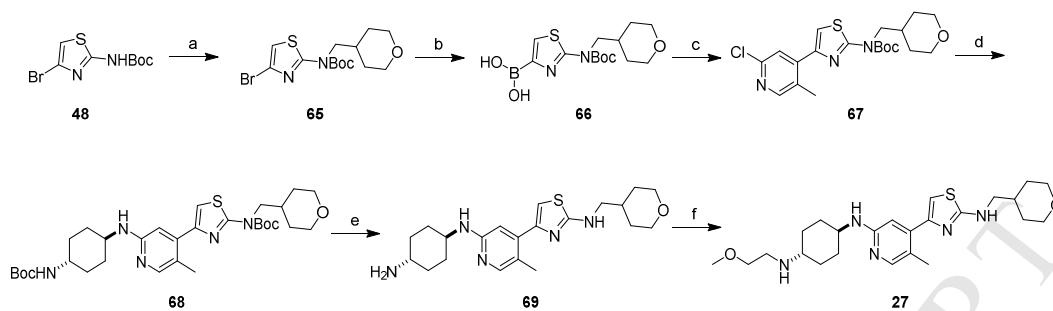
Scheme 3. Synthesis of Compounds **31, 33-34, 36** and **39-42**^a



^aReagents and conditions: (a) R³CH₂OH, PPh₃, DIAD, anhydrous THF, 0-40 °C, N₂, 1.5 h; (b) **45a**, Pd(PPh₃)₄, Na₂CO₃, DME/H₂O/dioxane, N₂, 70 °C, overnight; (c) **56c**, DIEA, DMSO, 100-110 °C, 2 days; (d) 1-bromo-2-(2-bromoethoxy)ethane, DBU, DMF, 85 °C, 3 h; (e) NaBH₄, DME/MeOH, 0 °C, 2 h; (f) **48**, PPh₃, DIAD, anhydrous THF, 0-40 °C, N₂, 1.5 h; (g) **56a-c**, DIEA, DMSO, 100-110 °C, 2 days.

Intermediate thiazol boronic acid **66** was obtained from **65** which was synthesized through Mitsunobu reaction between **48** and (tetrahydro-2*H*-pyran-4-yl)methanol. Following Suzuki coupling and Buchwald coupling reactions provided intermediate **68**. After removal of the N-Boc protecting group, final compound **27** was afforded through a nucleophilic substitution of **69** with 1-bromo-2-methoxyethane.

Scheme 4. Synthesis of Compound **27**^a



^aReagents and conditions: (a) (tetrahydro-2H-pyran-4-yl)methanol, PPh₃, DIAD, THF, -10-50 °C, 3 h; (b) bis(pinacolato)diboron, Pd(dppf)Cl₂·DCM, KOAc, dioxane, 100 °C, 3 h; (c) 4-bromo-2-chloro-5-methylpyridine, Pd(PPh₃)₄, K₃PO₄, dioxane, 100 °C, 4 h; (d) tert-butyl ((1*r*,4*r*)-4-aminocyclohexyl)carbamate, Pd₂(dba)₃, Binap, *t*BuONa, toluene, 120 °C, overnight; (e) TFA, DCM, rt, 1 h; (f) BrCH₂CH₂OCH₃, K₂CO₃, DMF, 100 °C, overnight.

In order to better explore the SAR of the inhibitors, besides the biochemical assay with CDK9 protein (IC₅₀), we also evaluated the inhibitor's cellular antiproliferative activity (GI₅₀) using MV4-11 (acute myeloid leukemia, AML) cell and MEC-1 (chronic lymphocytic leukemia, CLL) cell. In addition, we used normal Chinese hamster lung (CHL) cell to monitor the inhibitor's general cytotoxicity as well [29] (Table 1). We first prepared the pyridinthiazole compound **11**, which bears a Cl atom at R², a F atom at Y and a slightly bigger Boc group instead of methyl group attached to NH at X position. Unfortunately, it completely lost the activity against CDK9 kinase. Replacement of the NHBoc at X with NH-methylenetetrahydropyran moiety (**12**) started to gain back the activity to CDK9 (IC₅₀: 0.557 μM) but still did not show any cellular activity. Substitution of the F atom with 2-methoxyethanamine (Y = NH, R¹ = MeOCH₂CH₂) afforded **13**, which only showed weak activity against CDK9 and lacked the cellular

activity. Installation of the phenyl group at R¹ (**14**) slightly increased the activity to CDK9 (IC₅₀: 0.238 μM) but also displayed no cellular activity. When R¹ was the 4-fluoro benzoyl group (**15**), it resulted in significant activity loss to CDK9 and started to show general cytotoxicity. These results indicated that a more flexible group might be required at the R¹ position. We then tried to change the substituent group at R¹ to 4-amino cyclohexyl (**16**), which surprisingly showed good activity against CDK9 kinase (IC₅₀: 0.022 μM) and started to exhibit cellular activities in MV4-11 (GI₅₀: 0.14 μM) and MEC-1 (GI₅₀: 0.27 μM) cells. Meanwhile, it displayed good selectivity over normal CHL cells (GI₅₀: 3.5 μM). Addition of a methylene group between NH and 4-amino cyclohexyl (**17**) slightly decreased the activity to CDK9 (IC₅₀: 0.084 μM) and significantly lost the activity in the cellular assays. A series of acyl substitutions of the 4-amino cyclohexyl (**18-20**) were also examined but all led to activity loss to CDK9 kinase. However, aliphatic chain substitution at the same position such as methoxyethane (**21**) resulted in a potent activity against CDK9 (IC₅₀: 0.002 μM), although it also displayed weak cellular antiproliferative activity to cancer cell lines and cytotoxicity to CHL cells. Both of the methoxypropane (**22**) and ethoxyethane (**23**) substitution of the 4-amino cyclohexyl at R¹ caused slight activity loss to CDK9 kinase as well as the cellular activities. Interestingly, installation of a chiral center by introduction of (*S*)-1-methoxypropan-2-amine at R¹ position (**24**) completely lost the activity to CDK9 (IC₅₀: >10 μM), while the corresponding enantiomer (*R*)-1-methoxypropan-2-amine (**25**) started to gain back the activity (IC₅₀: 0.733 μM) although it was still much weaker than **21**. Replacement of the Cl in **21** with H atom (**26**) and methyl group (**27**) resulted in more than 50-fold and 126-fold activity loss to CDK9 indicating that the Cl atom might indeed form a halogen

bond interaction with Phe103 [28]. Change of the NH at X position of **21** to an O atom (**28**) or S atom (**29**) both led to activity loss (14 and 7-fold respectively) against CDK9 kinase.

Table 1. SAR Exploration Focused on the R¹/R²/X/Y Moieties^a



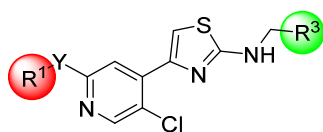
Compd.	R ¹	R ²	X	Y	CDK9 (IC ₅₀ : μM)	MV4-11 (GI ₅₀ : μM)	MEC-1 (GI ₅₀ : μM)	CHL (GI ₅₀ : μM)
11	-	Cl	NHBoc	F	>10	>10	>10	>10
12	-	Cl		F	0.557 ± 0.012	>10	>10	>10
13		Cl		NH	1.04 ± 0.012	>10	>10	>10
14		Cl		NH	0.238 ± 0.042	>10	>10	>10
15		Cl		NH	2.3 ± 0.233	0.55 ± 0.00 4	3.6 ± 0.023	0.93 ± 0.02 4
16		Cl		NH	0.022 ± 0.007	0.14 ± 0.033	0.27 ± 0.012	3.5 ± 0.027
17		Cl		NH	0.084 ± 0.008	1.9 ± 0.016	>10	3.9 ± 0.025

18		Cl		NH	0.101 ± 0.016	3.6 ± 0.042	>10	>10
19		Cl		NH	0.15 ± 0.013	>10	>10	>10
20		Cl		NH	1.89 ± 0.808	>10	>10	>10
21		Cl		NH	0.002 ± 0.0002	0.17 ± 0.045	1.24 ± 0.089	0.534 ± 0.087
22		Cl		NH	0.012 ± 0.008	1.09 ± 0.096	2.61 ± 0.214	2.03 ± 0.145
23		Cl		NH	0.051 ± 0.005	0.497 ± 0.014	0.634 ± 0.103	2.82 ± 0.241
24		Cl		NH	>10	0.44 ± 0.021	1.3 ± 0.015	3.6 ± 0.032
25		Cl		NH	0.733 ± 0.503	0.14 ± 0.031	0.31 ± 0.00 4	1.1 ± 0.018
26		H		NH	0.114 ± 0.014	0.91 ± 0.003	2.5 ± 0.014	1.2 ± 0.024
27		CH ₃		NH	0.253 ± 0.0 24	1.62 ± 0.098	3.56 ± 0.14	5.01 ± 0.11
28		Cl		NH	0.028 ± 0.006	0.57 ± 0.014	1.4 ± 0.023	3.3 ± 0.028
29		Cl		NH	0.014 ± 0.002	0.34 ± 0.025	0.8 ± 0.002	5.6 ± 0.045

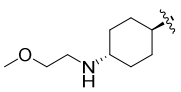
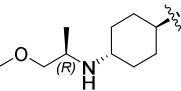
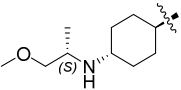
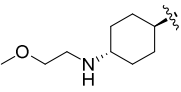
^aAll GI₅₀ values were obtained by triplet testing.

Because **21** exhibited potent inhibitory activity to CDK9 kinase in the biochemical assay but still lacked cell antiproliferative efficacy, we then fixed the R² group as Cl atom and the X moiety as NH and further explored the R¹/Y/R³ moieties (Table 2). Replacement of tetrahydropyran in **21** with H atom (**30**) at R³ decreased the activity to CDK9 about 50-fold indicating that a relatively large size group here might be favorable for the activity. A more hydrophobic CF₃ group at R³ position (**31**) gained back the activity against CDK9 to 0.017 μM (IC₅₀), although it still lacked potent antiproliferative activity in the cellular assays. Variation at the R³ site with different hydrophobic rings (**32-38**) all retained reasonable activities to CDK9 kinase but none of them exhibited potent cellular activity. When R³ was tetrahydrofuran group (**39**), it gained the activity to CDK9 with an IC₅₀ value of 0.09 μM and showed good selectivity window between normal cells and cancer cells, although it was still not very potent in the cellular assays. Interestingly, replacement of the R³ moiety with tetrahydropyran carbonitrile (**40**) resulted in great activity against CDK9 kinase (IC₅₀: 0.002 μM). In addition, it also exhibited potent antiproliferative efficacies in MV4-11 (GI₅₀: 0.012 μM) and MEC-1 (GI₅₀: 0.037 μM) cells, and meanwhile kept good selectivity over normal CHL cells (GI₅₀: 1.2 μM). Addition of a chiral center to the R¹ moiety of **40** by installation of (*R*)-1-methoxypropan-2-amine (**41**) almost retained both of the biochemical and cellular activities as well as the selectivity window. However, the corresponding *S* enantiomer (**42**) started to lose the cellular activities. Finally, changing NH at Y position of **21** to Oxygen atom (**43**) led to significant activity loss to CDK9 kinase.

Table 2. SAR Exploration Focused on the R¹/Y/R³ Moieties^a



Compd.	R ¹	R ³	Y	CDK9 (IC ₅₀ : μM)	MV4-11 (GI ₅₀ : μM)	MEC-1 (GI ₅₀ : μM)	CHL (GI ₅₀ : μM)
30		H	NH	0.101±0.0 16	0.53±0.01 2	1.4±0.023	1.9±0.035
31		CF ₃ -	NH	0.017±0.0 07	0.752±0.0 21	1.1±0.032	0.877±0.0 12
32			NH	0.096±0.0 44	0.74±0.01 6	0.89±0.03 3	1.4±0.021
33			NH	0.107±0.0 4	>10	2.26±0.10 1	1.29±0.08 5
34			NH	0.080±0.0 09	2.16±0.11 4	2.94±0.08 9	>10
35			NH	0.027±0.0 03	0.82±0.03 4	0.85±0.02 3	8±0.214
36			NH	0.094±0.0 04	3.46±0.14 5	6.31±0.12 1	2.04±0.09 8
37			NH	0.014±0.0 02	0.33±0.00 6	0.47±0.02 5	1±0.017
38			NH	0.002±0.0 001	0.88±0.05 3	0.45±0.03 2	1.1±0.041
39			NH	0.09±0.00 7	0.493±0.0 46	0.883±0.0 54	>10

40			NH	0.006±0.0 01	0.012±0.0 002	0.037±0.0 01	1.2±0.067
41			NH	0.009±0.0 002	0.014±0.0 024	0.047±0.0 036	1.1±0.017
42			NH	0.01±0.00 2	0.121±0.0 41	0.537±0.0 25	1.25±0.05 7
43			O	1.67±0.36 3	7.7±0.051	>10	>10

^aAll GI₅₀ values were obtained by triplet testing.

2.3. Selectivity profiling of compound **40**

Given the fact that **40** exhibited the best in vitro biochemical activity against CDK9 kinase, antiproliferative efficacy in cancer cell lines as well as the therapeutic window between normal cells and cancer cells, we then chose this compound for further selectivity evaluation. We first subjected **40** to Invitrogen's SelectScreen assay to examine its selectivity among structurally similar CDK kinase isoforms (Figure 4A-B). Among 10 different CDK isoforms which are available from the Invitrogen's platform, **40** only potently inhibited CDK9 kinase (IC₅₀: 0.001 μM) and exhibited more than 1000-fold selectivity over CDK1/2/3/5/7/8/11/14 and about 300-fold over CDK16. In order to investigate the inhibitor's selectivity among other protein kinases, we then tested **40** with DiscoverX's KINOMEScan technology for the kinomewide selectivity profiling [30]. Among 468 kinases/mutants, **40** exhibited a S score(1) of 0.01 at the concentration of 1 μM. Besides CDK9 kinase, it only showed strong binding to DYRK1A and DYRK1B kinases (Figure 4C-D, Supplemental table 1).

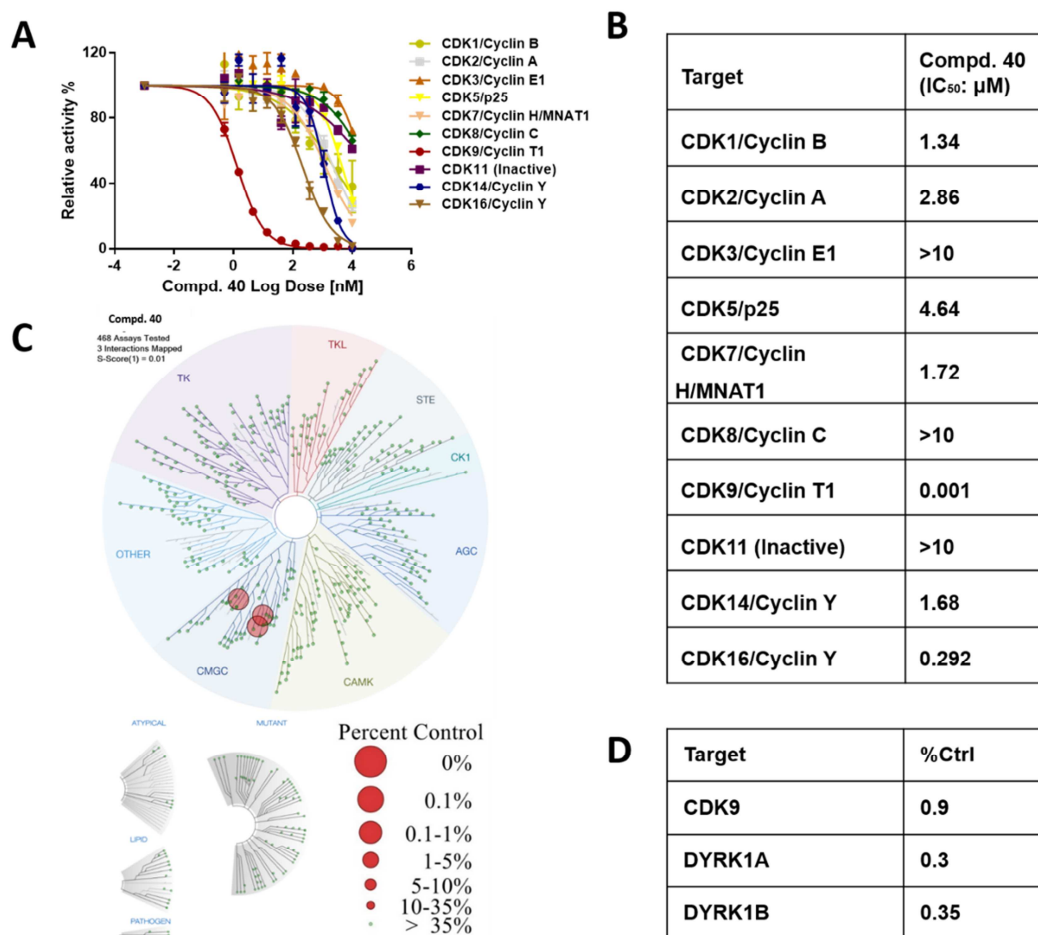


Figure 4. Selectivity profiling of compound **40**. (A, B) Biochemical testing of **40** against CDK isoforms with Invitrogen SelectScreen platform (Carlsbad, CA, USA). All data were obtained by triplet testing. (C) Treemap demonstration of kinome-wide selectivity of **40** with DiscoverX KINOMEScan technology. Measurements were performed at a concentration of 1 μ M of the inhibitor. The affinity was defined with respect to a DMSO control. (D) Targets that demonstrated strong binding to **40** in kinome profiling with a percent control number less than 1.

In order to better understand **40**'s binding mechanism, we next docked the inhibitor into the X-ray structure of CDK9 kinase (PDB ID: 4BCG) (Figure 5A). The modeling

results showed that the aminopyridine of **40** formed two hydrogen bonds with Cys106 in the hinge binding region. In the R¹ moiety, the oxygen atom formed a hydrogen bond with Asp109 located adjacent to that area. In addition, the NH at X position formed a hydrogen bond with Asp167 in the activation loop. Meanwhile, the CN group formed a hydrogen bond with the Thr29 in the P-loop. In comparison, it was disfavored when this binding mode was superimposed onto CDK7 kinase (PDB ID: 1UA2) (Figure 5B). First, Val100 adjacent to the hinge binding region of CDK7 prevented the methoxy group of the R¹ moiety from directing into this position due to the steric hindrance, while in CDK9 kinase the residue Gly122 at the same position lacks the isopropyl side chain of Val100 and thus avoid this interaction. In addition, the Thr29 in the CDK9 P-loop was replaced with Gly21 in the CDK7 P-loop, which lacks the capability to form hydrogen bond with the CN group of **40** in CDK7.

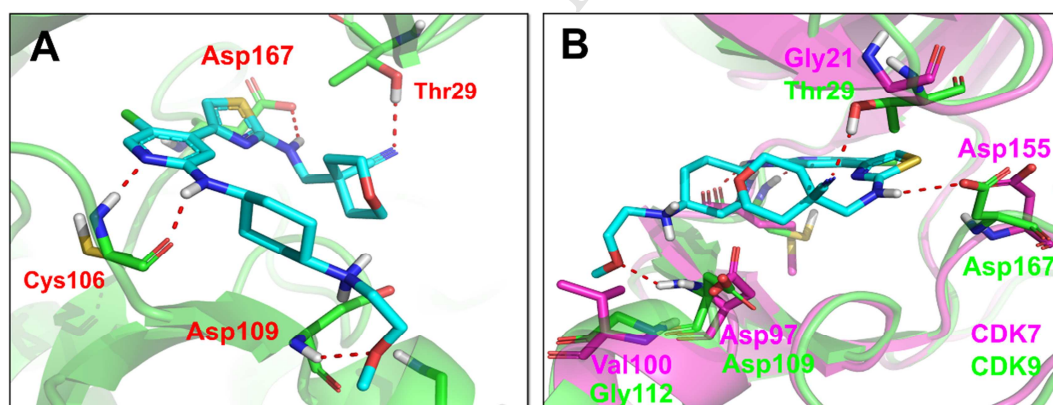


Figure 5. Binding mode of compound **40** with CDK9 kinase and superposition mode of CDK7 with CDK9 kinase. (A) Cartoon mode illustration of docking of **40** into CDK9 (PDB ID: 4BCG). (B) Illustration of the differences by overlaying CDK7 (PDB ID: 1UA2) and CDK9.

2.4. Cellular evaluation of compound **40**

We then examined the antiproliferative effect of **40** on a panel of established cancer cell lines (Table 3). Not surprisingly, it exhibited potent antiproliferative activities in solid tumor cell lines such as A375 (melanoma), A431 (squamous), BE(2)M17 (neuroblastoma), GIST-T1 (GIST) and COLO205 (colon cancer) with GI_{50} values from 0.002 to 0.044 μ M. In the leukemia cell lines including AML, CLL and B cell lymphoma cell lines, **40** also displayed strong growth inhibition efficacies with GI_{50} s ranging from single to double digit nM. In addition, **40** was much less sensitive in normal CHO cells (GI_{50} : 1.1 μ M) compared with the cancer cell lines. Compound **7**, which is a CDK1/2/5/9 multiple kinase inhibitor, also exhibited similar trends in these cancer cell lines except that it also showed relatively potent antiproliferative effect on CHO cells (GI_{50} : 0.16 μ M) which might reflect its multiple-target property.

Table 3. Antiproliferation Effects of Compound **40** on a Panel of Cancer Cell Lines^a

Cell line	Cell type	Compd. 40 (GI_{50} : μ M)	Compd. 7 (GI_{50} : μ M)
A375	melanoma	0.044±0.0023	0.011±0.0014
A431	squamous	0.019±0.0022	0.011±0.0011
BE(2)M17	neuroblastoma	0.034±0.0062	0.021±0.0013
GIST-T1	GIST	0.0021±0.0003	0.0088±0.0006
COLO205	colon cancer	0.014±0.0032	0.0068±0.0005
Ramos	B cell lymphoma	0.013±0.0015	0.0086±0.0007
HL-60	AML	0.056±0.0024	0.008±0.0003
MOLM13	AML	0.012±0.0011	0.0033±0.0004
MOLM14	AML	0.0011±0.0002	0.0045±0.0004
OCI-AML-3	AML	0.0066±0.0007	0.013±0.0021

SKM-1	AML	0.012±0.0018	0.011±0.0032
U937	AML	0.002±0.0003	0.01±0.0018
MEC-1	CLL	0.011±0.0034	0.0036±0.0006
MEC-2	CLL	0.037±0.0028	0.011±0.0029
CHO	Chinese hamster ovary cell	1.1±0.021	0.16±0.013

^aAll GI₅₀ values were obtained by triple testing.

Since CDK9 kinase inhibitors have been extensively evaluated for leukemia in the clinical trials, we chose MV4-11 (AML), HL-60 (AML) and MEC-1 (CLL) cell lines to examine **40**'s effects on the CDK9-mediated signaling pathways (Figure 6A). As expected, upon 2 h drug treatment, phospho-CDK9 Thr186 was not affected however phospho-RNA Pol II Ser2, which is the direct phosphorylation site in the CTD domain, was dose-dependently inhibited (EC₅₀: <100 nM) in all three cell lines. In addition, phospho-RNA pol II Ser5, which is the phosphorylation site of CDK7 was not affected even at 3 μM concentration of **40**, which again reflected its selectivity over CDK7 kinase. The expression level of antiapoptotic proteins such MCL-1 and c-MYC were dose-dependently reduced while other antiapoptotic proteins such as XIAP and BCL-2 were not affected upon 2 h treatment of **40** [31]. Compound **7** exhibited a similar trend. After 24 h drug treatment, by looking at the cleaved PARP and caspase-3 protein level, dose-dependent apoptosis was observed in all three cell lines which were in accordance with the observation of the antiapoptotic protein level reduction for MCL-1 and c-MYC (Figure 6B). Furthermore, the cell cycle was arrested at G0/G1 phase after 24 h treatment of **40**, indicating that the cells stopped growing after transcription was blocked (Figure 6C).

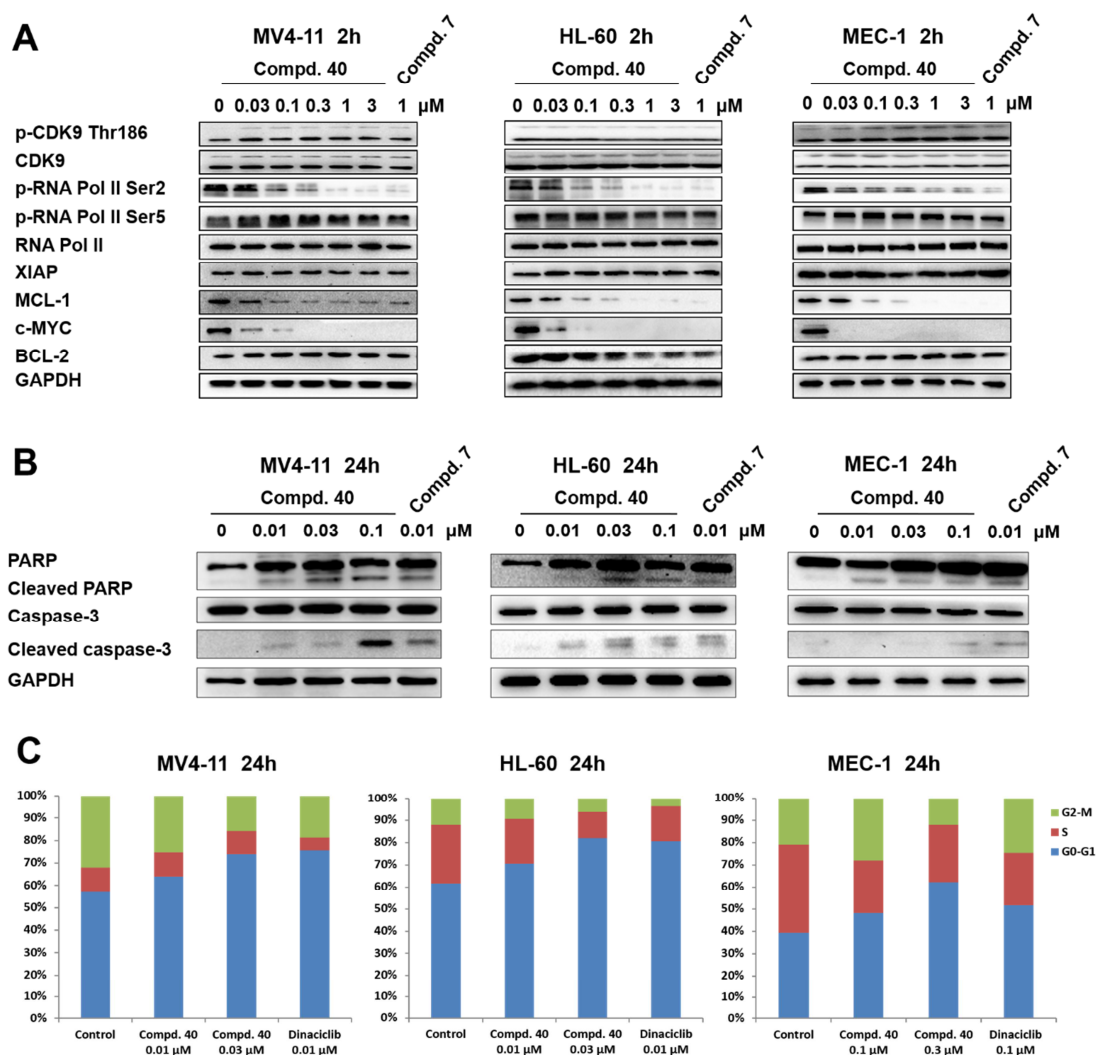


Figure 6. Cellular effects of compound **40** in AML cell lines MV4-11, HL-60 and CLL cell line MEC-1. (A) Effects of **40** on CDK9-mediated signaling pathways. (B) Effects of **40** on apoptosis. (C) Effects of **40** on cell cycle progression.

2.5. *In vivo* PK/PD evaluation of compound **40**

The PK properties of **40** were evaluated in different species including mice, Sprague-Dawley rats and beagle dogs through intravenous injection and oral administration (Table 5). The data showed that **40** was absorbed rapidly in dogs and mice

(T_{max} = 1.33 h and 2.00 h respectively) but slowly in rats (T_{max} = 3.33 h). **40** also displayed different half-lives in three different species via oral administration ($T_{1/2}$ = 1.55 h in mice, 3.37 h in rats and 20.37 h in dogs), which indicated that it was metabolized very slowly in dogs compared with mice and rats. The V_z values of **40** in mice, rats and dogs were 18203.84, 44464.14 and 12783.38 mL/kg respectively, indicating that it distributed widely in rats' body while mainly in blood and extracellular fluid for mice and dogs. In addition, **40** exhibited acceptable bioavailability in mice, rats and dogs (F = 45.01%, 45.10% and 39.15%, respectively). The PK properties indicated that **40** would be suitable for oral administration.

Table 5. Pharmacokinetic Study of Compound **40** in Mice, Sprague Dawley Rats and Beagle Dogs^a

Species	Mice (n = 24)		Rats (n = 3)		Dogs (n = 3)	
	iv (3 mg/kg)	po (10 mg/kg)	iv (3 mg/kg)	po (20 mg/kg)	iv (2 mg/kg)	po (10 mg/kg)
40						
$T_{1/2}$ (h)	1.72	1.55	6.80±0.47	3.37±0.45	13.14±2.63	20.37±17.09
T_{max} (h)	0.083	2.00	0.02±0.00	3.33±1.15	0.02±0.00	1.33±0.58
C_{max} (ng/mL)	573.36	115.76	1468.16±1 60.36	329.12±66.11	414.47±156 .82	770.55±259. 27
$AUC_{(0-t)}$ (h*ng/mL)	393.05	591.17	624.78±38 .42	1780.21± 341.34	2014.82±47 4.61	3943.59±18 19.29
$AUC_{(0-\infty)}$ (h*ng/mL)	408.01	612.21	662.30±47 .14	1989.38± 373.25	3121.69±12 21.56	16735.55±1 2152.92
V_z (mL/kg)	18203.84	--	44464.14± 469.28	--	12783.38±2 464.08	--
Cl (mL/h/kg)	7352.79	--	4545.22±3 28.14	--	711.30±277 .78	--

MRT _(0-t) (h)	1.25	3.24	4.69±0.13	9569.54± 2017.58	9.36±1.86	3.59±0.10
MRT _(0-∞) (h)	1.58	3.48	6.33±0.43	13311.12±23 12.20	20.36±7.04	29.25±24.28
F (%)	--	45.01	--	45.10±7.12	--	39.15±18.06

^aAll data were obtained by triple testing (±SD) except mice.

Finally, we tested **40**'s antitumor efficacy in MV4-11 cell-inoculated xenograft mouse model via oral administration (Figure 7A-B). Treatment of **40** at all dosages, *i.e.*, 10, 20 and 30 mg/kg/day, could almost completely suppress the tumor progression in the first two weeks and did not affect the animal's weight indicating that there was no general cytotoxicity at these doses. Interestingly, after stopped the treatment of **40**, the tumors of the animals treated with 10 mpk drug dosage started to grow again. However, this tumor recurrence was not observed in the 20 and 30 mpk dosage groups during the following week after administration of compound **40** was stopped and *p* values were quantified on the 21st day, which were 0.042, 0.0035 and 0.0028, respectively.

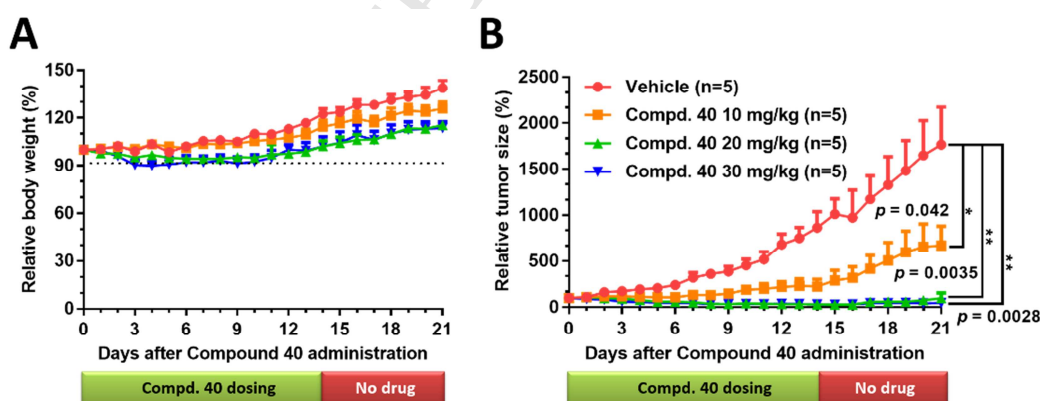


Figure 7. Compound **40**'s antitumor efficacy in MV4-11 xenograft mouse model. Female nu/nu mice bearing established MV4-11 tumor xenografts were treated with **40** at 10, 20, and 30 mg/kg/d dosage or vehicle. Daily oral administration was initiated when MV4-11

tumors had reached a size of 200–400 mm³. Each group contained five animals. Data, mean \pm SEM mpk, mg kg⁻¹ day⁻¹. (A) Body weight, and (B) Tumor size measurements from MV4-11 xenograft mice after **40** administration. Initial body weight and tumor size were set as 100%. *, $p < 0.05$. **, $p < 0.01$.

3. Conclusions

Starting from the core scaffold of CDK7/9 inhibitor **9**, a structure-guided drug design approach led to the discovery of a novel highly potent and selective CDK9 kinase inhibitor **40**. It exhibited single digit nM potency against CDK9 kinase in the biochemical assay. Compared to most of the currently known CDK kinase inhibitors, **40** achieved superior selectivity among CDK subfamily, especially the high selectivity between CDK9 and CDK7 kinase (over 1700-fold), both of which are critical transcription regulators. Therefore **40** would provide an ideal pharmacological tool for dissecting the CDK7- and CDK9-related physiology and pathology. In addition, **40** exhibited great antiproliferative activities in a range of established cancer cell lines including solid tumor and leukemia cells through inducing the apoptotic cell death. Meanwhile it showed a reasonable therapeutic window over normal cells, indicating that selective CDK9 kinase inhibitor might have potential antitumor efficacy in a wide range of the cancers. The impressive antitumor efficacy of **40** in the in vivo experiment especially that the tumor remained un-relapsed after stopping the drug treatment indicated a possible treatment-holiday-treatment drug application approach, which would provide a better therapeutic window and a more economical way for clinical usage. The high potency and selectivity, acceptable PK profile as well as good in vivo antitumor efficacy of **40** would make it a potential drug candidate for a range of cancers especially leukemias.

4. Experimental section

4.1. *Chemistry*. All reagents and solvents were purchased from commercial sources and used as obtained. ^1H NMR spectra were recorded with a Bruker 400 MHz NMR spectrometer and referenced to deuterated methanol (CD_3OD), deuterium dimethyl sulfoxide ($\text{DMSO-}d_6$) or deuterium chloroform (CDCl_3). Chemical shifts are expressed in ppm. In the NMR tabulation, s indicates singlet; d, doublet; t, triplet; q, quartet; m, multiplet; and br, broad peak. LC/MS experiments were performed on an Agilent 6224 TOF using an ESI source coupled to an Agilent 1260 Infinity HPLC system operating in reverse mode with an Agilent Eclipse Plus C18 1.8 μm , 3.0 mm \times 50 mm column. Flash column chromatography was conducted using silica gel (Silicycle 40–64 μm). The purities of all final compounds were determined to be above 95% by HPLC.

4.1.1. *tert-Butyl (4-(5-chloro-2-fluoropyridin-4-yl)thiazol-2-yl)carbamate (11)* A mixture of **48** (3.61 g, 12.9 mmol) and Na_2CO_3 (3.4 g, 32.3 mmol) in DME/ H_2O /dioxane (240/48/48 mL) was exchanged with N_2 twice, and 5-chloro-2-fluoro-4-(4,4,5,5-tetramethyl-1,3,2-dioxaborolan-2-yl)pyridine (**45a**) (6.6 g, 25.9 mmol) and $\text{Pd}(\text{PPh}_3)_4$ (1.45 g, 1.25 mmol) were added to the mixture. The reaction mixture was heated to 100 $^\circ\text{C}$ and stirred for 6 h under argon atmosphere. The solid was removed by centrifugation at 3000 rpm, 25 $^\circ\text{C}$ for 20 min. The supernatant was concentrated and the crude product was purified by silica gel flash chromatography (eluting with ethyl acetate in petroleum ether 2-5%) to give **11** as a white solid (1.57 g, yield = 37%). ^1H NMR (400 MHz, $\text{DMSO-}d_6$) δ 11.79 (s, 1H), 8.44 (s, 1H), 8.11 (s, 1H), 7.61 (s, 1H), 1.50 (s, 9H); LC/MS (ESI, m/z) 274.05 $[\text{M}+\text{H}]^+$.

4.1.2.

4-(5-Chloro-2-fluoropyridin-4-yl)-N-((tetrahydro-2H-pyran-4-yl)methyl)thiazol-2-amine (**12**) and *4-(5-chloro-2-((2-methoxyethyl)amino)pyridin-4-yl)-N-((tetrahydro-2H-pyran-4-yl)methyl)thiazol-2-amine* (**13**) (**53I**) (0.3 g, 0.71 mmol), 2-methoxyethan-1-amine (0.16 g, 2.1 mmol) and DIEA (0.36 g, 2.8 mmol) were dissolved in DMSO (10 mL) under N₂ protection and the reaction mixture was stirred at 100-110°C for two days. The resulting mixture was poured into cold water and extracted with ethyl acetate (3 × 20 mL) and washed with water (3 × 20 mL) and brine (20 mL). The combined organic layers were dried over anhydrous Na₂SO₄ and evaporated to dryness. The crude product was purified by silica gel flash chromatography (eluting with ethyl acetate in petroleum ether 2-5%) to give **12** (53 mg, yield = 23%) and **13** (0.33 g, yield = 43%) as white solid. Compound **12**, ¹H NMR (400 MHz, DMSO-*d*₆) δ 8.39 (s, 1H), 7.95 (s, 1H), 7.63 (s, 2H), 3.85 (s, 2H), 3.22 (s, 4H), 1.65-1.84 (m, 3H), 1.22 (s, 2H); LC/MS (ESI, m/z) 328.07 [M+H]⁺; Compound **13**, ¹H NMR (400 MHz, DMSO-*d*₆) δ 7.94 (s, 1H), 7.76 (s, 1H), 7.28 (s, 1H), 7.09 (s, 1H), 6.88 (s, 1H), 3.86 (s, 2H), 3.38-3.46 (m, 5H), 3.08-3.14 (m, 3H), 1.57-1.87 (m, 4H), 1.24 (s, 3H); LC/MS (ESI, m/z) 383.13 [M+H]⁺.

4.1.3. Compounds **14-15** were prepared following the synthetic procedure of **12/13** only the base DIEA was replaced with NaH. Compounds **21-26**, **30-43** were prepared following the synthetic procedure of **12/13**. Compounds **28** and **29** were prepared following the same procedure only the base DIEA was replaced with K₂CO₃.

4.1.3.1.

4-(5-Chloro-2-(phenylamino)pyridin-4-yl)-N-((tetrahydro-2H-pyran-4-yl)methyl)thiazol-

2-amine (14) Yield = 42%. $^1\text{H NMR}$ (400 MHz, $\text{DMSO-}d_6$) δ 9.27 (s, 1H), 8.19 (s, 1H), 7.80 (s, 1H), 7.63-7.65 (m, 2H), 7.22-7.47 (m, 4H), 6.92 (s, 1H), 3.86 (s, 2H), 1.64-1.85 (m, 4H), 1.24 (m, 4H). LC/MS (ESI, m/z) 401.12 $[\text{M}+\text{H}]^+$.

4.1.3.2.

N-(5-Chloro-4-(2-(((tetrahydro-2H-pyran-4-yl)methyl)amino)thiazol-4-yl)pyridin-2-yl)-4-fluorobenzamide (15) Yield = 8%. $^1\text{H NMR}$ (400 MHz, CDCl_3) δ 8.96 (s, 1H), 8.52 (s, 1H), 8.30 (s, 1H), 7.93-7.96 (m, 2H), 7.41 (s, 1H), 7.19 (t, $J = 8.4\text{Hz}$, 2H), 5.35-5.38 (m, 1H), 4.00-4.04 (m, 2H), 3.40-3.50 (m, 2H), 3.24 (t, $J = 6.4\text{Hz}$, 2H), 1.95-2.01 (m, 1H), 1.72-1.76 (m, 2H), 1.36-1.45 (m, 2H); LC/MS (ESI, m/z) 447.11 $[\text{M}+\text{H}]^+$.

4.1.3.3.

(1r,4r)-N¹-(5-Chloro-4-(2-(((tetrahydro-2H-pyran-4-yl)methyl)amino)thiazol-4-yl)pyridin-2-yl)-N⁴-(2-methoxyethyl)cyclohexane-1,4-diamine (21) Yield = 17%. $^1\text{H NMR}$ (400 MHz, CDCl_3) δ 8.06 (s, 1H), 7.33 (s, 1H), 6.96 (s, 1H), 5.65 (brs, 1H), 4.40 (d, $J = 8.0\text{Hz}$, 1H), 3.95-4.06 (m, 2H), 3.49-3.70 (m, 3H), 3.28-3.45 (m, 5H), 3.18 (t, $J = 6.4\text{Hz}$, 1H), 2.96-3.05 (m, 2H), 2.76-2.081 (m, 1H), 2.14-2.28 (m, 6H), 1.85-1.95 (m, .3H), 1.70-1.73 (m, 2H), 1.41-1.60 (m, 2H), 1.13-1.40 (m, 5H); LC/MS (ESI, m/z) 480.22 $[\text{M}+\text{H}]^+$.

4.1.3.4.

N¹-(5-Chloro-4-(2-(((tetrahydro-2H-pyran-4-yl)methyl)amino)thiazol-4-yl)pyridin-2-yl)-N⁴-(3-methoxypropyl)cyclohexane-1,4-diamine (22) Yield = 35%. $^1\text{H NMR}$ (400 MHz, $\text{DMSO-}d_6$) δ 7.99 (s, 1H), 7.75 (s, 1H), 7.28 (s, 1H), 7.03 (s, 1H), 6.76 (s, 1H), 3.86 (s, 2H), 3.63 (s, 1H), 3.41 (s, 2H), 3.20-3.29 (m, 7H), 2.96-3.04 (m, 3H), 2.06 (s, 4H), 1.86 (s, 3H), 1.64-1.66 (m, 2H), 1.45-1.47 (m, 2H), 1.21-1.27 (m, 4H); LC/MS (ESI, m/z) 494.24 $[\text{M}+\text{H}]^+$.

4.1.3.5.

*N*¹-(5-Chloro-4-(2-(((tetrahydro-2H-pyran-4-yl)methyl)amino)thiazol-4-yl)pyridin-2-yl)-*N*⁴-(2-ethoxyethyl)cyclohexane-1,4-diamine (**23**) Yield = 34%. ¹H NMR (400 MHz, CDCl₃) δ 8.06 (s, 1H), 7.29 (s, 1H), 6.96 (s, 1H), 6.29 (s, 1H), 4.75 (s, 1H), 3.99 (dd, *J* = 11.5, 4.2 Hz, 2H), 3.84 (t, *J* = 5.1 Hz, 2H), 3.55-3.67 (m, 4H), 3.38 (t, *J* = 11.7 Hz, 2H), 3.11-3.19 (m, 5H), 2.27 (dd, *J* = 28.0, 11.9 Hz, 4H), 1.66-1.85 (m, 5H), 1.25-1.39 (m, 6H); ¹³C NMR (212.5 MHz, CDCl₃) δ 169.08, 156.93, 148.28, 145.82, 140.97, 116.89, 108.44, 107.37, 67.56, 66.99, 66.70, 56.49, 52.31, 49.86, 45.00, 35.27, 31.40, 30.75, 29.25, 15.08; LC/MS (ESI, *m/z*) 494.24 [M+H]⁺.

4.1.3.6.

(1*r*,4*r*)-*N*¹-(5-Chloro-4-(2-(((tetrahydro-2H-pyran-4-yl)methyl)amino)thiazol-4-yl)pyridin-2-yl)-*N*⁴-((*S*)-1-methoxypropan-2-yl)cyclohexane-1,4-diamine (**24**) Yield = 4.3%. ¹H NMR (600 MHz, CDCl₃) δ 8.06 (s, 1H), 7.29 (s, 1H), 6.96 (s, 1H), 5.59 (brs, 1H), 4.36 (d, *J* = 8.0 Hz, 1H), 3.95-4.06 (m, 2H), 3.49-3.65 (m, 2H), 3.40-3.49 (m, 1H), 3.22-3.39 (m, 6H), 3.11-3.20 (m, 2H), 2.95-3.10 (m, 1H), 2.08-2.30 (m, 4H), 1.79-1.96 (m, 2H), 1.62-1.71 (m, 2H), 1.09-1.40 (m, 12H), 0.72-0.98 (m, 2H); LC/MS (ESI, *m/z*) 494.24 [M+H]⁺.

4.1.3.7.

(1*r*,4*r*)-*N*¹-(5-Chloro-4-(2-(((tetrahydro-2H-pyran-4-yl)methyl)amino)thiazol-4-yl)pyridin-2-yl)-*N*⁴-((*R*)-1-methoxypropan-2-yl)cyclohexane-1,4-diamine (**25**) Yield = 4.3%. ¹H NMR (400 MHz, CDCl₃) δ 8.06 (s, 1H), 7.33 (s, 1H), 6.96 (s, 1H), 5.30 (brs, 1H), 4.37 (d, *J* = 8.0 Hz, 1H), 3.99-4.03 (m, 2H), 3.52-3.59 (m, 1H), 3.25-3.49 (m, 4H), 3.36 (s, 3H), 3.16-3.25 (m, 2H), 3.06-3.10 (m, 1H), 2.60-2.65 (m, 1H), 2.16 (d, *J* = 10.8 Hz, 2H),

2.00-2.08 (m, 2H), 1.89-1.95 (m, 2H), 1.33-1.45 (m, 4H), 1.12-1.29 (m, 4H), 1.07 (d, $J = 6.4$ Hz, 3H); LC/MS (ESI, m/z) 494.24 $[M+H]^+$.

4.1.3.8.

(1r,4r)-N¹-(2-Methoxyethyl)-N⁴-(4-(2-(((tetrahydro-2H-pyran-4-yl)methyl)amino)thiazol-4-yl)pyridin-2-yl)cyclohexane-1,4-diamine (26) Yield = 17%. ¹H NMR (400 MHz, CDCl₃) δ 7.95-8.02 (m, 1H), 6.79-6.89 (m, 3H), 5.48 (brs, 1H), 4.65-4.85 (m, 1H), 3.98-4.01 (m, 2H), 3.57-3.61 (m, 3H), 3.35-3.42 (m, 5H), 3.18-3.20 (m, 2H), 2.89-2.92 (m, 2H), 2.61-2.68 (m, 1H), 2.17-2.27 (m, 3H), 2.04-2.08 (m, 3H), 1.87-1.96 (m, 1H), 1.69-1.73 (m, 2H), 1.20-1.50 (m, 10H), 0.79-0.95 (m, 2H); LC/MS (ESI, m/z) 446.26 $[M+H]^+$.

4.1.3.9.

(1r,4r)-N¹-(5-Chloro-4-(2-(((tetrahydro-2H-pyran-4-yl)methoxy)thiazol-4-yl)pyridin-2-yl)-N⁴-(2-methoxyethyl)cyclohexane-1,4-diamine (28) Yield = 25.3%. ¹H NMR (400 MHz, CDCl₃) δ 8.07 (s, 1H), 7.50 (s, 1H), 6.95 (s, 1H), 4.39 (d, $J = 8.0$ Hz, 1H), 4.31 (d, $J = 6.4$ Hz, 2H), 4.03 (dd, $J_1 = 3.2$ Hz, $J_2 = 11.2$ Hz, 2H), 3.59-3.61 (m, 1H), 3.54 (t, $J = 4.8$ Hz, 2H), 3.44-3.47 (m, 2H), 3.37 (s, 3H), 2.85 (t, $J = 5.2$ Hz, 2H), 2.53-2.54 (m, 1H), 2.15-2.18 (m, 3H), 2.00-2.03 (m, 2H), 1.73-1.76 (m, 2H), 1.46-1.52 (m, 2H), 1.15-1.37 (m, 5H); LC/MS (ESI, m/z) 481.20 $[M+H]^+$.

4.1.3.10.

(1r,4r)-N¹-(5-Chloro-4-(2-(((tetrahydro-2H-pyran-4-yl)methyl)thio)thiazol-4-yl)pyridin-2-yl)-N⁴-(2-methoxyethyl)cyclohexane-1,4-diamine (29) Yield = 34.5%. ¹H NMR (400 MHz, CDCl₃) δ 8.07 (s, 1H), 7.98 (s, 1H), 6.99 (s, 1H), 4.42 (brs, 1H), 3.91-4.10 (m, 2H), 3.55-3.71 (m, 3H), 2.83-3.52 (m, 12H), 2.13-2.17 (m, 4H), 1.95-2.05 (m, 1H), 1.69-1.87

(m, 2H), 1.31-1.56 (m, 5H), 1.02-1.35 (m, 4H), 0.79-0.95 (m, 1H); LC/MS (ESI, m/z) 497.18 [M+H]⁺.

4.1.3.11.

(1*r*,4*r*)-*N*¹-(5-Chloro-4-(2-(methylamino)thiazol-4-yl)pyridin-2-yl)-*N*⁴-(2-methoxyethyl)cyclohexane-1,4-diamine (**30**) Yield = 68%. ¹H NMR (400 MHz, DMSO-*d*₆) δ 7.97 (s, 1H), 7.61-7.62 (m, 1H), 7.29 (s, 1H), 7.04 (s, 1H), 6.70 (d, *J* = 7.6 Hz, 1H), 3.59-3.61 (m, 2H), 3.37-3.42 (m, 3H), 3.25 (s, 3H), 2.87 (d, *J* = 4.8 Hz, 2H), 2.74-2.77 (m, 2H), 1.90-1.96 (m, 4H), 1.12-1.23 (m, 4H); LC/MS (ESI, m/z) 396.16 [M+H]⁺.

4.1.3.12.

*N*¹-(5-Chloro-4-(2-((2,2,2-trifluoroethyl)amino)thiazol-4-yl)pyridin-2-yl)-*N*⁴-(2-methoxyethyl)cyclohexane-1,4-diamine (**31**) Yield = 32%. ¹H NMR (400 MHz, DMSO-*d*₆) δ 8.33 (s, 1H), 8.01 (s, 1H), 7.43 (s, 1H), 7.04 (s, 1H), 6.77 (s, 1H), 4.22 (s, 2H), 3.61 (s, 3H), 3.02-3.12 (m, 3H), 2.03-2.11 (m, 4H), 1.45-1.48 (m, 2H), 1.25-1.27 (m, 5H); LC/MS (ESI, m/z) 464.15 [M+H]⁺.

4.1.3.13.

(1*r*,4*r*)-*N*¹-(5-Chloro-4-(2-((cyclopropylmethyl)amino)thiazol-4-yl)pyridin-2-yl)-*N*⁴-(2-methoxyethyl)cyclohexane-1,4-diamine (**32**) Yield = 35%. ¹H NMR (400 MHz, DMSO-*d*₆) δ 7.97 (s, 1H), 7.84 (t, *J* = 5.6 Hz, 1H), 7.28 (s, 1H), 7.04 (s, 1H), 7.74 (d, *J* = 8.0 Hz, 2H), 3.52-3.55 (m, 3H), 3.29 (s, 3H), 3.17 (t, *J* = 6.4 Hz, 2H), 2.94 (brs, 1H), 2.70-2.85 (m, 1H), 1.97-2.01 (m, 4H), 1.18-1.23 (m, 5H), 0.46-0.49 (m, 2H), 0.23-0.24 (m, 2H); LC/MS (ESI, m/z) 436.19 [M+H]⁺.

4.1.3.14.

*N*¹-(5-Chloro-4-(2-((cyclobutylmethyl)amino)thiazol-4-yl)pyridin-2-yl)-*N*⁴-(2-methoxyethyl)cyclohexane-1,4-diamine (**33**) Yield = 30%. ¹H NMR (400 MHz, DMSO-*d*₆) δ 7.97 (s, 1H), 7.84 (t, *J* = 5.6 Hz, 1H), 7.28 (s, 1H), 7.04 (s, 1H), 7.74 (d, *J* = 8.0 Hz, 2H), 3.52-3.55 (m, 3H), 3.29 (s, 3H), 3.17 (t, *J* = 6.4 Hz, 2H), 2.94 (brs, 1H), 2.70-2.85 (m, 1H), 1.97-2.01 (m, 4H), 1.18-1.23 (m, 5H), 0.46-0.49 (m, 2H), 0.23-0.24 (m, 2H); LC/MS (ESI, m/z) 436.19 [M+H]⁺.

yl)cyclohexane-1,4-diamine (**33**) Yield = 40%. ¹H NMR (400 MHz, DMSO-*d*₆) δ 7.98 (s, 1H), 7.69 (s, 1H), 7.26 (s, 1H), 7.02 (s, 1H), 3.60 (s, 1H), 3.43 (s, 2H), 3.26-3.27 (m, 5H), 2.80 (s, 2H), 2.58-2.61 (m, 2H), 1.72-2.03 (m, 10H), 1.18 (s, 4H); LC/MS (ESI, m/z) 450.21 [M+H]⁺.

4.1.3.15.

*N*¹-(5-Chloro-4-(2-((cyclopentylmethyl)amino)thiazol-4-yl)pyridin-2-yl)-*N*⁴-(2-methoxyethyl)cyclohexane-1,4-diamine (**34**) Yield = 42%. ¹H NMR (400 MHz, CDCl₃) δ 8.03 (s, 1H), 7.28 (s, 1H), 6.95 (s, 1H), 5.71 (s, 1H), 4.55 (s, 1H), 3.77-3.79 (m, 2H), 3.61-3.64 (m, 2H), 3.39 (s, 3H), 3.01-3.16 (m, 5H), 2.16-2.29 (m, 5H), 1.54-1.84 (m, 9H), 1.19-1.23 (m, 2H); LC/MS (ESI, m/z) 464.23 [M+H]⁺.

4.1.3.16.

(1*r*,4*r*)-*N*¹-(5-Chloro-4-(2-((cyclohexylmethyl)amino)thiazol-4-yl)pyridin-2-yl)-*N*⁴-(2-methoxyethyl)cyclohexane-1,4-diamine (**35**) Yield = 30%. ¹H NMR (400 MHz, DMSO-*d*₆) δ 7.97 (s, 1H), 7.67-7.69 (m, 1H), 7.25 (s, 1H), 7.01 (s, 1H), 6.71 (d, *J* = 7.6 Hz, 1H), 3.50-3.53 (m, 1H), 3.36-3.47 (m, 2H), 3.13 (t, *J* = 6.0 Hz, 2H), 2.94-2.97 (m, 2H), 2.72-2.81 (m, 1H), 1.99-2.02 (m, 4H), 1.61-1.77 (m, 5H), 1.19-1.33 (m, 7H), 0.91-1.01 (m, 2H); LC/MS (ESI, m/z) 478.24 [M+H]⁺.

4.1.3.17.

*N*¹-(4-(2-(((1*r*,5*R*,7*S*)-Adamantan-2-yl)methyl)amino)thiazol-4-yl)-5-chloropyridin-2-yl)-*N*⁴-(2-methoxyethyl)cyclohexane-1,4-diamine (**36**) Yield = 12%. ¹H NMR (400 MHz, CDCl₃) δ 8.00 (s, 1H), 7.28 (s, 1H), 6.98 (s, 1H), 5.83 (s, 1H), 4.79 (s, 1H), 3.80-3.82 (m, 2H), 3.63-3.69 (m, 1 H), 3.38 (s, 3H), 3.07-3.19 (m, 4H), 2.90 (d, *J* = 5.2 Hz, 2H),

2.20-2.32 (m, 5H), 1.99 (s, 3H), 1.54-1.85 (m, 10H), 1.46 (s, 2H), 1.17-1.21 (m, 1H);
LC/MS (ESI, m/z) 530.27 [M+H]⁺.

4.1.3.18.

(1*r*,4*r*)-*N*¹-(4-(2-(Benzylamino)thiazol-4-yl)-5-chloropyridin-2-yl)-*N*⁴-(2-methoxyethyl)cyclohexane-1,4-diamine (**37**) Yield = 30%. ¹H NMR (400 MHz, DMSO-*d*₆) δ 8.21 (t, *J* = 6.0 Hz, 1H), 7.98 (s, 1H), 7.26-7.40 (m, 6H), 7.05 (s, 1H), 6.72 (d, *J* = 7.6 Hz, 1H), 4.52 (d, *J* = 5.6 Hz, 2H), 3.46-3.53 (m, 4H), 2.97 (brs, 2H), 2.81 (brs, 1H), 1.99-2.01 (m, 4H), 1.18-1.34 (m, 4H); LC/MS (ESI, m/z) 472.19 [M+H]⁺.

4.1.3.19.

(1*r*,4*r*)-*N*¹-(5-Chloro-4-(2-((4-fluorobenzyl)amino)thiazol-4-yl)pyridin-2-yl)-*N*⁴-(2-methoxyethyl)cyclohexane-1,4-diamine (**38**) Yield = 30%. ¹H NMR (400 MHz, DMSO-*d*₆) δ 8.22-8.24 (m, 1H), 7.98 (s, 1H), 7.41-7.44 (m, 2H), 7.32 (s, 1H), 7.18 (t, *J* = 8.8 Hz, 2H), 7.04 (s, 1H), 6.73 (d, *J* = 7.6 Hz, 1H), 4.50 (d, *J* = 5.6 Hz, 2H), 3.52-3.55 (m, 3H), 3.29 (s, 3H), 2.96 (brs, 2H), 2.97 (brs, 1H), 1.98-2.01 (m, 4H), 1.21-1.23 (m, 4H); LC/MS (ESI, m/z) 490.18 [M+H]⁺.

4.1.3.20.

*N*¹-(5-Chloro-4-(2-(((tetrahydrofuran-3-yl)methyl)amino)thiazol-4-yl)pyridin-2-yl)-*N*⁴-(2-methoxyethyl)cyclohexane-1,4-diamine (**39**) Yield = 35%. ¹H NMR (400 MHz, CDCl₃) δ 8.06 (s, 1H), 7.30 (s, 1H), 6.97 (s, 1H), 6.08 (s, 1H), 4.72 (s, 1H), 3.82-3.96 (m, 2H), 3.74-3.3.79 (m, 3H), 3.62-3.68 (m, 3H), 3.40 (s, 3H), 3.29 (t, *J* = 6.1 Hz, 2H), 3.14 (t, *J* = 5.1 Hz, 2H), 3.01-3.07 (m, 1H), 2.60-2.67 (m, 1H), 2.24 (t, *J* = 16.6 Hz, 4H), 2.06-2.15 (m, 1H), 1.66-1.75 (m, 3H), 1.18-1.21 (m, 1H); LC/MS (ESI, m/z) 466.20 [M+H]⁺.

4.1.3.21.

*4-(((4-(5-Chloro-2-(((1*r*,4*r*)-4-((2-methoxyethyl)amino)cyclohexyl)amino)pyridin-4-yl)thiazol-2-yl)amino)methyl)tetrahydro-2*H*-pyran-4-carbonitrile (40)* Yield = 28%. ¹H NMR (400 MHz, CDCl₃) δ 8.06 (s, 1H), 7.40 (s, 1H), 6.98 (s, 1H), 5.51 (t, *J* = 6.4 Hz, 1H), 4.43 (d, *J* = 8.0 Hz, 1H), 4.00-4.04 (m, 2H), 3.60-3.73 (m, 7H), 3.36 (s, 3H), 3.07 (d, *J* = 5.2 Hz, 2H), 2.89 (brs, 1H), 2.14-2.24 (m, 4H), 1.94-1.98 (m, 2H), 1.76-1.83 (m, 2H), 1.54-1.57 (m, 2H), 1.26-1.29 (m, 3H); ¹³C NMR (125 MHz, CDCl₃) δ 167.53, 156.91, 148.39, 145.61, 140.45, 121.78, 116.72, 109.76, 107.77, 68.98, 64.49, 58.87, 56.43, 52.88, 49.80, 45.05, 39.64, 33.00, 31.28, 29.17; LC/MS (ESI, *m/z*) 505.22 [M+H]⁺.

4.1.3.22.

*4-(((4-(5-Chloro-2-(((1*R*,4*r*)-4-(((*R*)-1-methoxypropan-2-yl)amino)cyclohexyl)amino)pyridin-4-yl)thiazol-2-yl)amino)methyl)tetrahydro-2*H*-pyran-4-carbonitrile (41)* Yield = 19.1%. ¹H NMR (400 MHz, CDCl₃) δ 8.06 (s, 1H), 7.38 (s, 1H), 6.97 (s, 1H), 5.92 (brs, 1H), 4.45 (d, *J* = 8.0 Hz, 1H), 4.02 (dd, *J*₁ = 2.8 Hz, *J*₂ = 12 Hz, 2H), 3.71-3.74 (m, 4H), 3.54-3.56 (m, 1H), 3.35 (s, 3H), 3.21-3.25 (m, 2H), 3.00-3.05 (m, 1H), 2.50-2.60 (m, 1H), 2.15 (d, *J* = 9.6 Hz, 2H), 2.04-2.07 (m, 1H), 1.95 (d, *J* = 12.8 Hz, 3H), 1.74-1.82 (m, 3H), 1.10-1.30 (m, 4H), 1.00 (d, *J* = 8.4 Hz, 3H); LC/MS (ESI, *m/z*) 519.23 [M+H]⁺.

4.1.3.23.

*4-(((4-(5-Chloro-2-(((1*S*,4*r*)-4-(((*S*)-1-methoxypropan-2-yl)amino)cyclohexyl)amino)pyridin-4-yl)thiazol-2-yl)amino)methyl)tetrahydro-2*H*-pyran-4-carbonitrile (42)* Yield = 22%. ¹H NMR (400 MHz, DMSO-*d*₆) δ 8.12 (t, *J* = 6.0 Hz, 1H), 7.98 (s, 1H), 7.35 (s, 1H), 7.03 (s, 1H), 6.69 (d, *J* = 8.0 Hz, 1H), 3.91-3.95 (m, 2H), 3.66 (d, *J* = 6.4 Hz, 2H),

3.55-3.65 (m, 1H), 3.47-3.51 (m, 3H), 3.29 (s, 3H), 3.17 (d, $J = 4.8$ Hz, 1H), 1.86-1.99 (m, 6H), 1.66-1.74 (m, 2H), 0.99-1.26 (m, 8H); LC/MS (ESI, m/z) 519.23 $[M+H]^+$.

4.1.3.24.

*4-(5-Chloro-2-(((1*r*,4*r*)-4-((2-methoxyethyl)amino)cyclohexyl)oxy)pyridin-4-yl)-N-((tetrahydro-2*H*-pyran-4-yl)methyl)thiazol-2-amine (43)* Yield = 22%. ^1H NMR (400 MHz, CDCl_3) δ 8.13 (s, 1H), 7.34 (s, 1H), 7.29 (s, 1H), 5.30-5.33 (m, 1H), 4.90-4.96 (m, 1H), 4.01 (dd, $J_1 = 3.6$ Hz, $J_2 = 11.2$ Hz, 2H), 3.52 (t, $J = 5.2$ Hz, 2H), 3.37-3.43 (m, 5H), 3.24 (t, $J = 6.4$ Hz, 2H), 2.83 (t, $J = 5.2$ Hz, 2H), 2.52-2.57 (m, 1H), 2.16-2.18 (m, 2H), 2.00-2.02 (m, 2H), 1.87-1.94 (m, 1H), 1.68-1.72 (m, 2H), 1.25-1.53 (m, 7H); LC/MS (ESI, m/z) 481.20 $[M+H]^+$.

4.1.4.

*(1*r*,4*r*)-*N*¹-(5-Chloro-4-(2-(((tetrahydro-2*H*-pyran-4-yl)methyl)amino)thiazol-4-yl)pyridin-2-yl)cyclohexane-1,4-diamine (16)* **53l** (0.3 g, 0.71 mmol), *tert*-butyl ((1*r*,4*r*)-4-aminocyclohexyl)carbamate (0.16 g, 2.1 mmol) and DIEA (0.36 g, 2.8 mmol) were dissolved in DMSO (10 mL) under N_2 protection and the reaction mixture was stirred at 100-110 °C for two days. The resulting mixture was poured into cold water and extracted with ethyl acetate (3×20 mL) and washed with water (3×20 mL) and brine (20 mL). The combined organic layers were dried over anhydrous Na_2SO_4 and evaporated to dryness. The crude product was purified by flash chromatography (eluting with ethyl acetate in petroleum ether 2-5%) to give a white solid, which was then dissolved in DCM (5 mL), placed at 0 °C and charged with TFA (5 mL). The mixture was stirred for approximately 2 h. Then it was concentrated to dryness, basified with sat. NaHCO_3 until $\text{pH} = 10$ and diluted with ethyl acetate (3×20 mL). The organic layers

were dried over anhydrous Na_2SO_4 and then evaporated to dryness. The residue was purified by silica gel flash chromatography (eluting with MeOH in DCM 5%) to give the title compound **16** as a white solid (79 mg, yield = 30%). ^1H NMR (400 MHz, CDCl_3) δ 8.06 (s, 1H), 7.33 (s, 1H), 6.96 (s, 1H), 5.21-5.30 (m, 1H), 4.32 (d, $J = 8.0\text{Hz}$, 1H), 3.99-4.03 (m, 2H), 3.53-3.61 (m, 1H), 3.38-3.44 (m, 2H), 3.23 (t, $J = 6.4\text{Hz}$, 2H), 2.68-2.74 (m, 1H), 2.11-2.13 (m, 2H), 1.85-2.13 (m, 3H), 1.70-1.73 (m, 2H), 1.10-1.45 (m, 7H); ^{13}C NMR (212.5 MHz, CDCl_3) δ 168.59, 157.17, 148.39, 146.07, 140.63, 116.56, 108.59, 107.63, 77.18, 77.03, 76.88, 67.55, 52.04, 50.17, 50.08, 35.33, 35.26, 32.05, 30.72. LC/MS (ESI, m/z) 422.18 $[\text{M}+\text{H}]^+$.

4.1.5. Compound **17** was prepared following the synthetic procedure of **16**.

*4-(2-(((1*r*,4*r*)-4-Aminocyclohexyl)methyl)amino)-5-chloropyridin-4-yl)-N-((tetrahydro-2*H*-pyran-4-yl)methyl)thiazol-2-amine (**17**)* Yield = 34.8%. ^1H NMR (400 MHz, CD_3OD) δ 7.82 (s, 1H), 7.11 (s, 1H), 6.95 (s, 1H), 3.84-3.88 (m, 2H), 3.32 (t, $J = 11.2\text{Hz}$, 2H), 3.16-3.17 (m, 2H), 3.16 (d, $J = 6.8\text{ Hz}$, 2H), 3.04 (d, $J = 6.8\text{ Hz}$, 2H), 2.75-2.80 (m, 1H), 1.81-1.92 (m, 5H), 1.61-1.64 (m, 2H), 1.49-1.51 (m, 1H), 1.12-1.29 (m, 5H), 0.92-1.05 (m, 2H); LC/MS (ESI, m/z) 436.19 $[\text{M}+\text{H}]^+$.

4.1.6.

*N-((1*r*,4*r*)-4-((5-Chloro-4-(2-(((tetrahydro-2*H*-pyran-4-yl)methyl)amino)thiazol-4-yl)pyridin-2-yl)amino)cyclohexyl)acetamide (**18**)* To a solution of **16** (100 mg, 0.24 mmol) in DCM (5 mL) at 0 °C was added acetyl chloride (28 mg, 0.35 mmol) dropwise. After 1 h until the reaction was complete, the mixture was evaporated to dryness and the crude product was purified by silica gel flash chromatography (eluting with MeOH in DCM 5%) to give the title compound **18** as a white solid (41 mg, yield = 41%). ^1H NMR (400

MHz, CDCl₃) δ 8.06 (s, 1H), 7.33 (s, 1H), 6.96 (s, 1H), 5.30-5.34 (m, 1H), 5.20-5.30 (m, 1H), 4.32 (d, $J = 8.0$ Hz, 1H), 3.99-4.03 (m, 2H), 3.78-3.83 (m, 1H), 3.62-3.64 (m, 1H), 3.41 (t, $J = 12$ Hz, 2H), 3.24 (t, $J = 6.4$ Hz, 1H), 2.13-2.15 (m, 2H), 2.00-2.09 (m, 2H), 1.95 (s, 3H), 1.70-1.73 (m, 2H), 1.20-1.49 (m, 7H); LC/MS (ESI, m/z) 464.19 [M+H]⁺.

4.1.7. Compounds **19-20** were prepared following the synthetic procedure of **18**.

4.1.7.1.

N-(4-((5-Chloro-4-(2-(((tetrahydro-2H-pyran-4-yl)methyl)amino)thiazol-4-yl)pyridin-2-yl)amino)cyclohexyl)cyclopropanecarboxamide (**19**) Yield = 34%. ¹H NMR (400 MHz, DMSO-*d*₆) δ 7.97-7.81 (m, 2H), 7.82 (s, 1H), 7.36 (s, 1H), 7.14 (s, 1H), 3.86 (s, 2H), 3.54-3.62 (m, 3H), 3.21-3.29 (m, 5H), 1.97 (s, 2H), 1.83 (s, 3H), 1.63-1.67 (m, 2H), 1.52 (s, 1H), 1.26 (s, 4H), 0.63 (s, 4H); LC/MS (ESI, m/z) 490.20 [M+H]⁺.

4.1.7.2.

N-(4-((5-Chloro-4-(2-(((tetrahydro-2H-pyran-4-yl)methyl)amino)thiazol-4-yl)pyridin-2-yl)amino)cyclohexyl)-2-methoxyacetamide (**20**) Yield = 8%. ¹H NMR (400 MHz, DMSO-*d*₆) δ 7.99 (s, 1H), 7.77 (s, 1H), 7.59 (s, 1H), 7.29 (s, 1H), 7.05 (s, 1H), 3.85-3.88 (m, 2H), 3.75-3.79 (m, 2H), 3.61 (s, 2H), 3.20-3.31 (m, 7H), 1.92-1.99 (m, 2H), 1.76-1.84 (m, 3H), 1.64-1.67 (m, 2H), 1.39-1.43 (m, 2H), 1.18-1.29 (m, 4H); LC/MS (ESI, m/z) 494.20 [M+H]⁺.

4.1.8.

(1*r*,4*r*)-*N*1-(2-Methoxyethyl)-*N*4-(5-methyl-4-(2-(((tetrahydro-2H-pyran-4-yl)methyl)amino)thiazol-4-yl)pyridin-2-yl)cyclohexane-1,4-diamine (**27**) To a solution of **69** (65 mg, 0.16 mmol) in DMF (5 mL) was added K₂CO₃ (24 mg, 0.18 mmol) and 1-bromo-2-methoxyethane (22 mg, 0.18 mmol). The mixture was stirred at 100 °C

overnight and water (25 mg, 0.18 mmol) was added. The mixture was extracted with EA (3 × 10 mL). The combined organic layers were washed with brine (10 mL) and dried over anhydrous Na₂SO₄. The organic layers were evaporated to dryness and the crude product was purified by silica gel flash chromatography (eluting with MeOH in DCM 6%) to give the title compound **27** as a white solid (20 mg, 27%). ¹H NMR (500 MHz, DMSO-*d*₆) δ 7.78 (s, 1H), 7.68 (t, *J* = 5.6 Hz, 1H), 6.78 (s, 1H), 6.73 (s, 1H), 6.13 (d, *J* = 7.8 Hz, 1H), 3.87-3.84 (m, 2H), 3.62-3.57 (m, 1H), 3.47 (t, *J* = 5.4 Hz, 2H), 3.30-3.25 (m, 6H), 3.17 (t, *J* = 6.2 Hz, 2H), 2.87 (t, *J* = 5.5 Hz, 2H), 2.64-2.63 (m, 1H), 2.21 (s, 3H), 1.99-1.94 (m, 4H), 1.88-1.81 (m, 1H), 1.65-1.61 (m, 2H), 1.26-1.13 (m, 6H); ¹³C NMR (125 MHz, CDCl₃) δ 169.4, 157.0, 149.5, 149.2, 143.4, 119.3, 106.4, 105.5, 70.7, 67.7, 59.0, 56.7, 52.3, 50.3, 45.9, 35.3, 31.9, 30.8, 30.7, 17.6; LC/MS (ESI, *m/z*) 460.27 [M+H]⁺.

4.1.9. *5-Chloro-2-fluoro-4-(4,4,5,5-tetramethyl-1,3,2-dioxaborolan-2-yl)pyridine (45a)* A solution of (5-chloro-2-fluoropyridin-4-yl)boronic acid (**44**) (0.7 g, 4.46 mmol) and pinacol (0.63 g, 5.35 mmol) in toluene (50 mL) was refluxed overnight. The reaction mixture was concentrated to give the crude product, which was purified by silica gel flash chromatography (eluting with petroleum ether) to give **45a** as a white solid (0.92 g, yield = 80%). ¹H NMR (400 MHz, CDCl₃) δ 8.17 (s, 1H), 7.20 (s, 1H), 1.37 (s, 12H); LC/MS (ESI, *m/z*) 258.09 [M+H]⁺.

4.1.10. *tert-Butyl (5-bromothiazol-2-yl)carbamate (47)* To a solution of 5-bromothiazol-2-amine (**46**) (105 g, 403.1 mmol) in THF (500 mL) was added DMAP (2.41 g, 20 mmol) and the solution became turbid. Then a solution of Boc₂O (105.6 g, 484.6 mmol) in THF (50 mL) was added to the above mixture slowly and the resulting

mixture was stirred at room temperature for 2 days. The reaction mixture was concentrated and the crude product was purified by silica gel flash chromatography (eluting with ethyl acetate in petroleum ether 10–17%) to give **47** as an off-white solid (45.1 g, yield = 40%). ^1H NMR (400 MHz, CDCl_3) δ 11.75 (br, 1H), 7.24 (s, 1H), 1.58 (s, 9H); LC/MS (ESI, m/z) 222.98 $[\text{M}+\text{H}-56]^+$.

4.1.11. *tert-Butyl (4-bromothiazol-2-yl)carbamate (48)* To a solution of diisopropylamine (64 mL, 446 mmol) in THF (100 mL) was added dropwise *n*-BuLi (2.5 M, 173 mL) under N_2 atmosphere at 0 °C. After that a solution of **47** (40 g, 143.9 mmol) in THF (400 mL) was added dropwise at 0 °C. The reaction mixture was stirred at the same temperature for 2 h, and then quenched with sat. NH_4Cl (500 mL) and extracted with ethyl acetate (3 \times 300 mL). The combined organic layers were washed with brine (100 mL) and dried over anhydrous Na_2SO_4 . The organic layers were evaporated to dryness and the crude product was purified by silica gel flash chromatography (eluting with ethyl acetate in petroleum ether 1–30%) to give the title compound **48** as a white solid (31.2 g, yield = 78%). ^1H NMR (400 MHz, CDCl_3) δ 8.05 (br, 1H), 6.78 (s, 1H), 1.56 (s, 9H); LC/MS (ESI, m/z) 222.98 $[\text{M}+\text{H}-56]^+$.

4.1.12. *Methyl 4-cyanotetrahydro-2H-pyran-4-carboxylate (50)* To a solution of methyl 2-cyanoacetate (**49**) (39.1 g, 395.3 mmol) and 1-bromo-2-(2-bromoethoxy)ethane (100 g, 434.8 mmol) in DMF (600 mL) was added DBU (90 g, 593 mmol) and the reaction mixture was heated to 85 °C for 3 h. After the reaction was complete as determined by TLC, the solid was filtered off and washed twice with ethyl acetate (150 mL \times 2). The mother liquor was concentrated to brown oil. Colorless oil was collected under reduced pressure at 65–70 °C, then turned into white solid after cooling down to provide **50** (42.1

g, yield = 62.8%). ^1H NMR (400 MHz, CDCl_3) δ 3.05-4.00 (m, 2H), 3.86 (s, 3H), 3.59-3.75 (m, 2H), 2.11-2.18 (m, 2H), 2.00-2.03 (m, 2H); LC/MS (ESI, m/z) 170.08 $[\text{M}+\text{H}]^+$.

4.1.13. *4-(Hydroxymethyl)tetrahydro-2H-pyran-4-carbonitrile (51)* To a solution of **50** (42 g, 248.4 mmol) in DME/methanol (400 mL/40 mL) at 0 °C was added NaBH_4 (411.1 g, 149 mmol) in batches. The reaction mixture was stirred at room temperature for 16 h. The resulting mixture was quenched by saturated NH_4Cl and extracted with ethyl acetate (100 mL \times 3). The combined organic layers were dried over anhydrous Na_2SO_4 and evaporated to dryness. The residue was purified by silica gel flash chromatography (eluting with ethyl acetate in petroleum ether 10–30%) to give the product **51** as a pale yellow oil (28.1 g, yield = 79.5%). ^1H NMR (400 MHz, CDCl_3) δ 3.99-4.02 (m, 2H), 3.66-3.74 (m, 4H), 2.64-2.66 (br, 1H), 1.89-1.93 (m, 2H), 1.60-1.68 (m, 2H); LC/MS (ESI, m/z) 142.09 $[\text{M}+\text{H}]^+$.

4.1.14. *tert-Butyl*

(4-bromothiazol-2-yl)((4-cyanotetrahydro-2H-pyran-4-yl)methyl)carbamate (52a) To a solution of **51** (0.5 g, 1.8 mmol), **48** (0.381 g, 2.7 mmol) and triphenylphosphine (0.707 g, 2.7 mmol) in anhydrous THF (20 mL) at 0 °C was added diisopropyl azodicarboxylate (DIAD) (0.545 g, 2.7 mmol) dropwise. The reaction mixture was allowed to stir at room temperature for 10 mins and then stirred at 40 °C overnight. The resulting mixture was concentrated and the residue was purified by silica gel flash chromatography (eluting with ethyl acetate in petroleum ether 2-5%) to give the product **52a** as a white solid (0.365 g, yield = 50%). ^1H NMR (400 MHz, CDCl_3) δ 6.84 (s, 1H), 4.38 (s, 2H),

3.93-3.97 (m, 2H), 3.65-3.72 (m, 2H), 1.77-1.90 (m, 4H), 1.61 (s, 9H); LC/MS (ESI, m/z) 346.05 [M+H-56]⁺.

4.1.15. Compounds **52b-f** were prepared following the synthetic procedure of **52a**.

4.1.15.1. *tert-Butyl (4-bromothiazol-2-yl)(2,2,2-trifluoroethyl)carbamate (52b)* Yield = 87%. ¹H NMR (400 MHz, CDCl₃) δ 6.87 (s, 1H), 4.80-4.84 (m, 2H), 1.58 (s, 9H); LC/MS (ESI, m/z) 304.98 [M+H-56]⁺.

4.1.15.2. *tert-Butyl (4-bromothiazol-2-yl)(cyclobutylmethyl)carbamate (52c)* Yield = 85%. ¹H NMR (400 MHz, CDCl₃) δ 6.78 (s, 1H), 4.11 (d, *J* = 6.9 Hz, 2H), 2.73-2.80 (m, 1H), 1.95-2.03 (m, 2H), 1.77-1.87 (m, 4H), 1.57 (s, 9H); LC/MS (ESI, m/z) 291.04 [M+H-56]⁺.

4.1.15.3. *tert-Butyl (4-bromothiazol-2-yl)(cyclopentylmethyl)carbamate (52d)* Yield = 75%. ¹H NMR (400 MHz, CDCl₃) δ 6.97 (s, 1H), 4.02 (d, *J* = 7.6 Hz, 2H), 2.35-2.44 (m, 2H), 1.64-1.72 (m, 4H), 1.52-1.59 (m, 10H), 1.25-1.32 (m, 2H); LC/MS (ESI, m/z) 305.06 [M+H-56]⁺.

4.1.15.4. *tert-Butyl (((1*r*,5*R*,7*S*)-adamantan-2-yl)methyl)(4-bromothiazol-2-yl)carbamate (52e)* Yield = 75%. ¹H NMR (400 MHz, CDCl₃) δ 6.97 (s, 1H), 3.93 (s, 2H), 1.94 (s, 3H), 1.52-1.69 (m, 21H); LC/MS (ESI, m/z) 371.11 [M+H-56]⁺.

4.1.15.5. *tert-Butyl (4-bromothiazol-2-yl)((tetrahydrofuran-3-yl)methyl)carbamate (52f)* Yield = 73%. ¹H NMR (400 MHz, CDCl₃) δ 6.81 (s, 1H), 4.16 (dd, *J* = 13.8, 7.4 Hz, 2H), 4.06 (dd, *J* = 13.8, 7.3 Hz, 1H), 3.89-3.94 (m, 1H), 3.75-3.82 (m, 1H), 3.57-3.60 (m, 1H), 2.78-2.85 (m, 1H), 1.95-2.03 (m, 1H), 1.66-1.75 (m, 1H), 1.57 (s, 9H); LC/MS (ESI, m/z) 307.04 [M+H-56]⁺.

4.1.16. *tert-Butyl*

(4-(5-chloro-2-fluoropyridin-4-yl)thiazol-2-yl)((4-cyanotetrahydro-2H-pyran-4-yl)methyl)carbamate (**53a**) A mixture of **52a** (5.2 g, 12.9 mmol) and Na₂CO₃ (3.4 g, 32.3 mmol) in DME/H₂O/dioxane (240/48/48 mL) was exchanged with N₂ twice, then **45a** (6.6 g, 25.9 mmol) and Pd(PPh₃)₄ (1.45 g, 1.25 mmol) were added to the above mixture. The reaction mixture was heated to 100 °C and stirred for 6 h under argon atmosphere. The solid was removed by centrifugation at 3000 rpm, 25 °C for 20 min. The supernatant was concentrated and the residue was purified by silica gel flash chromatography (eluting with ethyl acetate in petroleum ether 2-5%) to give the product **53a** as a white solid (3.2 g, yield = 55%). ¹H NMR (400 MHz, CDCl₃) δ 8.26 (s, 1H), 7.98 (s, 1H), 7.61 (d, 1H), 4.47 (s, 2H), 3.95-4.00 (m, 2H), 3.69-3.76 (m, 2H), 1.87-1.89 (m, 4H), 1.65 (s, 9H); LC/MS (ESI, m/z) 397.12 [M+H-56]⁺.

4.1.17. Compounds **53b-f** were prepared following the synthetic procedure of **53a**.

4.1.17.1. *tert-Butyl*

(4-(5-chloro-2-fluoropyridin-4-yl)thiazol-2-yl)(2,2,2-trifluoroethyl)carbamate (**53b**) Yield = 83%. ¹H NMR (400 MHz, CDCl₃) δ 8.25 (s, 1H), 8.00 (s, 1H), 7.62 (d, *J* = 2.0 Hz, 1H), 4.90 (q, *J* = 8.3 Hz, 2H), 1.61 (s, 9H); LC/MS (ESI, m/z) 356.05 [M+H-56]⁺.

4.1.17.2. *tert-Butyl*

(4-(5-chloro-2-fluoropyridin-4-yl)thiazol-2-yl)(cyclobutylmethyl)carbamate (**53c**) Yield = 75%. ¹H NMR (400 MHz, CDCl₃) δ 8.24 (s, 1H), 7.95 (s, 1H), 7.67 (s, 1H), 4.21 (d, *J* = 6.9 Hz, 2H), 2.80-2.86 (m, 1H), 2.01-2.07 (m, 2H), 1.83-1.91 (m, 4H), 1.60 (s, 9H); LC/MS (ESI, m/z) 342.11 [M+H-56]⁺.

4.1.17.3. *tert-Butyl*

(4-(5-chloro-2-fluoropyridin-4-yl)thiazol-2-yl)(cyclopentylmethyl)carbamate (**53d**) Yield = 80%. ¹H NMR (400 MHz, CDCl₃) δ 8.24 (s, 1H), 7.96 (s, 1H), 7.67 (s, 1H), 4.12 (d, *J* = 7.2 Hz, 2H), 2.43-2.50 (m, 1H), 1.67-1.75 (m, 4H), 1.55-1.62 (m, 11H), 1.32-1.39 (m, 2H); LC/MS (ESI, m/z) 356.13 [M+H-56]⁺.

4.1.17.4. *tert-Butyl*

((1*r*,5*R*,7*S*)-adamantan-2-yl)methyl(4-(5-chloro-2-fluoropyridin-4-yl)thiazol-2-yl)carbamate (**53e**) Yield = 60%. ¹H NMR (400 MHz, CDCl₃) δ 8.23 (s, 1H), 7.98 (s, 1H), 7.68 (s, 1H), 4.03 (s, 2H), 1.95 (s, 3H), 1.53-1.70 (m, 21H); LC/MS (ESI, m/z) 422.17 [M+H-56]⁺.

4.1.17.5. *tert-Butyl*

(4-(5-chloro-2-fluoropyridin-4-yl)thiazol-2-yl)((tetrahydrofuran-3-yl)methyl)carbamate (**53f**) Yield = 76%. ¹H NMR (400 MHz, CDCl₃) δ 8.25 (s, 1H), 7.98 (s, 1H), 7.64 (s, 1H), 4.15-4.28 (m, 2H), 3.93-3.98 (m, 1H), 3.78-3.85 (m, 2H), 3.63-3.67 (m, 1H), 2.83-2.90 (m, 1H), 2.00-2.09 (m, 1H), 1.73-1.81 (m, 1H), 1.61 (s, 9H); LC/MS (ESI, m/z) 358.11 [M+H-56]⁺.

4.1.18. *tert-Butyl* (4-(5-chloro-2-fluoropyridin-4-yl)thiazol-2-yl)(methyl)carbamate (**53g**) **11** (0.59 g, 1.8 mmol), MeOH (0.086 g, 2.7 mmol) and triphenylphosphine (0.71 g, 2.7 mmol) were dissolved in anhydrous THF (20 mL) at 0 °C. To the above mixture was added diisopropyl azodicarboxylate (DIAD) (0.55 g, 2.7 mmol) dropwise. The reaction mixture was allowed to stir at room temperature for 10 mins and then stirred at 40°C overnight. The resulting mixture was concentrated and the residue was purified by silica gel flash chromatography (eluting with ethyl acetate in petroleum ether 2-5%) to

give the product **53g** as a white solid (0.37 g, yield = 50%). ¹H NMR (400 MHz, CDCl₃) δ 8.24 (s, 1H), 7.96 (s, 1H), 7.73 (d, *J* = 1.6 Hz, 1H), 3.62 (s, 3H), 1.61 (s, 9H); LC/MS (ESI, *m/z*) 288.06 [M+H]⁺.

4.1.19. Compound **53h-l** was prepared following the synthetic procedure of **53g**.

4.1.19.1. *tert*-Butyl

(4-(5-chloro-2-fluoropyridin-4-yl)thiazol-2-yl)(cyclopropylmethyl)carbamate (**53h**) Yield = 73%. ¹H NMR (400 MHz, CDCl₃) δ 8.24 (s, 1H), 7.96 (s, 1H), 7.67 (d, *J* = 1.2 Hz, 1H), 4.07 (d, *J* = 4.8 Hz, 2H), 1.61 (s, 9H), 1.37-1.39 (m, 1H), 0.45-0.54 (m, 4H); LC/MS (ESI, *m/z*) 328.09 [M+H]⁺.

4.1.19.2. *tert*-Butyl

(4-(5-chloro-2-fluoropyridin-4-yl)thiazol-2-yl)(cyclohexylmethyl)carbamate (**53i**) Yield = 70%. ¹H NMR (400 MHz, CDCl₃) δ 8.24 (s, 1H), 7.95 (s, 1H), 7.65 (d, *J* = 1.6 Hz, 1H), 4.02 (d, *J* = 7.2 Hz, 2H), 1.88-1.92 (m, 2H), 1.59-1.74 (m, 5H), 1.59 (s, 9H), 1.10-1.28 (m, 2H), 1.05-1.10 (m, 2H); LC/MS (ESI, *m/z*) 370.14 [M+H]⁺.

4.1.19.3. *tert*-Butyl benzyl(4-(5-chloro-2-fluoropyridin-4-yl)thiazol-2-yl)carbamate (**53j**) Yield = 64%. ¹H NMR (400 MHz, CDCl₃) δ 8.23 (s, 1H), 7.98 (s, 1H), 7.63 (d, *J* = 1.6 Hz, 1H), 7.26-7.38 (m, 5H), 5.37 (s, 2H), 1.53 (s, 9H); LC/MS (ESI, *m/z*) 364.09 [M+H]⁺.

4.1.19.4. *tert*-Butyl

(4-(5-chloro-2-fluoropyridin-4-yl)thiazol-2-yl)(4-fluorobenzyl)carbamate (**53k**) Yield = 71%. ¹H NMR (400 MHz, CDCl₃) δ 8.24 (s, 1H), 7.97 (s, 1H), 7.62 (d, *J* = 0.8 Hz, 1H), 7.35-7.38 (m, 2H), 6.99-7.02 (m, 2H), 5.33 (s, 2H), 1.55 (s, 9H); LC/MS (ESI, *m/z*) 382.09 [M+H]⁺.

4.1.19.5. *tert*-Butyl

(4-(5-chloro-2-fluoropyridin-4-yl)thiazol-2-yl)((tetrahydro-2H-pyran-4-yl)methyl)carbamate (**53l**) Yield = 71%. ¹H NMR (400 MHz, CDCl₃) δ 8.25 (s, 1H), 7.96 (s, 1H), 7.62 (s, 1H), 4.01-4.15 (m, 2H), 3.95-3.99 (m, 2H), 3.32-3.39 (m, 2H), 2.14-2.24 (m, 1H), 1.52-1.77 (m, 11H), 1.40-1.51 (m, 2H); LC/MS (ESI, m/z) 372.13 [M+H]⁺.

4.1.19.6.

tert-Butyl

(4-(2-chloropyridin-4-yl)thiazol-2-yl)((tetrahydro-2H-pyran-4-yl)methyl)carbamate (**53m**) Yield = 61%. LC/MS (ESI, m/z) 410.13 [M+H]⁺.

4.1.20. (*S*)-1-Methoxypropan-2-yl 4-methylbenzenesulfonate (**55a**) A mixture of NaH (9.52 g, 238 mmol) in THF (200 mL) was added (*S*)-1-methoxypropan-2-ol (21 g, 233 mmol) dropwise at 0 °C. The reaction mixture was stirred at room temperature for 1.5 h, and then TosCl (45.3 g, 230 mmol) in THF (200 mL) was added while the temperature was kept below 10 °C. The reaction mixture was then stirred at room temperature overnight. The resulting mixture was quenched with water (20 mL) and extracted with ethyl acetate (200 mL × 3). The combine organic layers were concentrated and the residue was purified by silica gel flash chromatography (eluting with ethyl acetate in petroleum ether 5-15%) to give the product **55a** as a yellow solid (37.1 g, yield = 65.1%). ¹H NMR (400 MHz, CDCl₃) δ 7.81 (d, 2H), 7.33 (d, 2H), 4.67-4.74 (m, 1H), 3.30-3.44 (m, 2H), 3.24(s, 3H), 2.44 (s, 3H), 1.27 (d, 3H); LC/MS (ESI, m/z) 245.08 [M+H]⁺.

4.1.21. Compound **55b** was prepared following the synthetic procedure of **55a**.

(*R*)-1-Methoxypropan-2-yl 4-methylbenzenesulfonate (**55b**) Yield = 82%. ¹H NMR (400 MHz, CDCl₃) δ 7.81 (d, 2H), 7.33 (d, 2H), 4.67-4.74 (m, 1H), 3.30-3.44 (m, 2H), 3.24(s, 3H), 2.44 (s, 3H), 1.27 (d, 3H); LC/MS (ESI, m/z) 245.08 [M+H]⁺.

4.1.22. *(1r,4S)-N¹-((R)-1-Methoxypropan-2-yl)cyclohexane-1,4-diamine (56a)* **55a** (5 g, 20.5 mmol) and (1r,4r)-cyclohexane-1,4-diamine (5.84 g, 51.2 mmol) were dissolved in CH₃CN (50 mL) and the mixture was allowed to stir at 90 °C overnight. The solid was washed with DCM (50 mL × 3). The combine organic layers were concentrated and the crude product was purified by silica gel flash chromatography (eluting with methanol in dichloromethane 5-15%) to give **56a** as a yellow liquid (2.5 g, yield = 65%). ¹H NMR (400 MHz, CDCl₃) δ 3.44 (s, 1H), 3.34 (s, 3H), 3.27-3.31 (m, 1H), 3.20-3.24 (m, 1H), 2.97-3.04 (m, 1H), 2.62-2.68 (m, 1H), 2.46-2.52 (m, 1H), 1.94-1.99 (m, 1H), 1.84-1.90 (m, 3H), 1.06-1.18 (m, 3H), 1.01 (d, 3H); LC/MS (ESI, m/z) 187.18 [M+H]⁺.

4.1.23. Compound **56b** was prepared following the synthetic procedure of **56a**.

(1r,4R)-N¹-((S)-1-Methoxypropan-2-yl)cyclohexane-1,4-diamine (56b) Yield = 68%. ¹H NMR (400 MHz, CDCl₃) δ 3.44 (s, 1H), 3.34 (s, 3H), 3.27-3.31 (m, 1H), 3.20-3.24 (m, 1H), 2.97-3.04 (m, 1H), 2.62-2.68 (m, 1H), 2.46-2.52 (m, 1H), 1.94-1.99 (m, 1H), 1.84-1.90 (m, 3H), 1.06-1.18 (m, 3H), 1.01 (d, 3H); LC/MS (ESI, m/z) 187.18 [M+H]⁺.

4.1.24. *(1r,4r)-N¹-(2-Methoxyethyl)cyclohexane-1,4-diamine hydrochloride (56c)* *tert*-Butyl ((1r,4r)-4-aminocyclohexyl)carbamate (10 g, 46.7 mmol), 1-bromo-2-methoxyethane (5.22 g, 37.4 mmol) and K₂CO₃ (12.9 g, 93.4 mmol) were dissolved in CH₃CN (150 mL), and then the reaction mixture was heated to 80 °C for 16 h. The solid was washed with DCM (50 mL × 3). The combine organic layers were concentrated and the residue was purified by flash chromatography (eluting with MeOH in DCM 5%) to give a white solid, which was then dissolved in ethyl acetate (10 mL) and charged with 4 N HCl in ethyl acetate (10 mL) at 0 °C. The mixture was stirred for approximately 3 h. The solid was filtered to afford the desired product **56c** as a white

solid (8.3 g, yield = 65%). ^1H NMR (400 MHz, $\text{DMSO-}d_6$) δ 9.08 (brs, 2H), 8.24 (brs, 3H), 3.63 (t, $J = 5.2$ Hz, 2H), 3.30 (s, 3H), 3.07-3.10 (m, 2H), 2.91-2.95 (m, 2H), 2.12-2.15 (m, 2H), 2.02-2.05 (m, 2H), 1.37-1.47 (m, 4H); LC/MS (ESI, m/z) 173.17 $[\text{M}+\text{H}]^+$.

4.1.25. Compounds **56d-e** were prepared following the synthetic procedure of **56c**.

4.1.25.1. *(1r,4r)-N¹-(3-Methoxypropyl)cyclohexane-1,4-diamine (56d)* Yield = 63%. ^1H NMR (400 MHz, CD_3OD) δ 3.54 (t, $J = 5.8$ Hz, 2H), 3.37 (s, 3H), 3.15-3.21 (m, 4H), 2.24 (d, $J = 21.9$ Hz, 4H), 1.97-2.02 (m, 2H), 1.54-1.61 (m, 4H); LC/MS (ESI, m/z) 187.18 $[\text{M}+\text{H}]^+$.

4.1.25.2. *(1r,4r)-N¹-(2-Ethoxyethyl)cyclohexane-1,4-diamine (56e)* Yield = 64%. ^1H NMR (400 MHz, CD_3OD) δ 3.71-3.74 (m, 2H), 3.61 (q, $J = 6.9$ Hz, 1H), 3.26-3.28 (m, 2H), 3.18-3.21 (m, 2H), 2.24 (dd, $J = 36.7, 9.8$ Hz, 4H), 1.51-1.65 (m, 4H), 1.25 (t, $J = 7.1$ Hz, 3H); LC/MS (ESI, m/z) 187.18 $[\text{M}+\text{H}]^+$.

4.1.26. *4-(Bromomethyl)tetrahydro-2H-pyran (58)* To a solution of **57** (8.12 g, 10 mmol) and *N*-bromobutanamide (NBS) (13.71 g, 248 mmol) in DCM (400 mL) was added PPh_3 (20.17 g, 248 mmol) at 0 °C. The reaction mixture was stirred at room temperature for 1-2 h. The resulting mixture was washed with water (20 mL) and brine (3×20 mL). The organic layer was concentrated and the residue was purified by silica gel flash chromatography (eluting with ethyl acetate in petroleum ether 2-5%) to give the product **58** as a colorless oil (6.2 g, yield = 49%). ^1H NMR (400 MHz, CDCl_3) δ 3.98 (dd, $J = 11.2$ Hz, 4.4 Hz, 2H), 3.37 (td, $J = 12.0$ Hz, 1.6 Hz, 2H), 3.28 (d, $J = 6.4$ Hz, 2H), 1.91-1.84 (m, 1H), 1.76 (d, $J = 13.2$ Hz, 2H), 1.35 (qd, $J = 12.4$ Hz, 4.4 Hz, 2H); LC/MS (ESI, m/z) 179.01 $[\text{M}+\text{H}]^+$.

4.1.27. *(Tetrahydro-2H-pyran-4-yl)methyl ethanethioate (59)* A mixture of **58** (3 g, 16.75 mmol) and potassium thioacetate CH₃COSK (3.4 g, 33.5 mmol) in DMF (60 mL) was stirred at 90 °C for 2 h. The reaction mixture was poured into cold water and then extracted with ethyl acetate (3 × 30 mL). The combined organic layers were washed with water (3 × 60 mL) and brine (30 mL), and then dried over anhydrous MgSO₄ and evaporated to dryness. The crude product was purified by silica gel flash chromatography (eluting with ethyl acetate in petroleum ether 2-5%) to give the title compound **59** as a yellow oil, (1.8 g, yield = 69%). ¹H NMR (400 MHz, CDCl₃) δ 3.94 (dd, *J* = 11.6 Hz, 4.4 Hz, 2H), 3.36-3.33 (m, 2H), 2.81 (d, *J* = 6.4 Hz, 2H), 2.32 (s, 3H), 1.69-1.65 (m, 3H), 1.30 (qd, *J* = 12.4 Hz, 4.0 Hz, 2H); LC/MS (ESI, *m/z*) 175.08 [M+H]⁺.

4.1.28. *(Tetrahydro-2H-pyran-4-yl)methanethiol (60)* To a solution of **59** (0.895 g, 5 mmol) in anhydrous THF (20 mL) was added LiAlH₄ (0.22 g, 5 mmol) in batches at 0 °C under N₂ atmosphere. The reaction mixture was stirred at room temperature overnight. The resulting mixture was diluted with THF (50 mL) and Na₂SO₄ (1.42 g, 10 mmol) was added slowly and the mixture was stirred for 10 min. The supernatant was concentrated to give the crude product **60** as a yellow oil (0.68 g, yield = 100%), which was used in the next step without further purification. ¹H NMR (400 MHz, CDCl₃) δ 3.98 (dd, *J* = 11.2 Hz, 3.6 Hz, 2H), 3.42-3.34 (m, 2H), 2.63 (d, *J* = 6.8 Hz, 2H), 1.90-1.84 (m, 1H), 1.79-1.75 (m, 2H), 1.37-1.28 (m, 3H); LC/MS (ESI, *m/z*) 133.07 [M+H]⁺.

4.1.29. *4-Bromo-2-(((tetrahydro-2H-pyran-4-yl)methyl)thio)thiazole (61)* To a solution of **59** (0.632 g, 4.8 mmol) in THF (30 mL) was added NaH (0.2 g, 4.8 mmol) at 0 °C and the reaction mixture was stirred at room temperature for 10 min. A solution of 2,4-dibromothiazole (0.964 g, 4 mmol) in THF (10 mL) was added to the above mixture

dropwise and the reaction mixture was stirred overnight. The resulting mixture was bleached with saturated NH_4Cl (20 mL) and extracted with ethyl acetate (3×30 mL). The combined organic layers were dried over anhydrous Na_2SO_4 and concentrated under reduced pressure. The residue was purified by silica gel flash chromatography (eluting with ethyl acetate in petroleum ether 4%) to afford **61** as an off-white solid (0.7 g, yield = 60%). ^1H NMR (400 MHz, CDCl_3) δ 7.07 (s, 1H), 3.98 (dd, $J = 11.2$ Hz, 4.4 Hz, 2H), 3.37 (td, $J = 11.8$ Hz, 2.0 Hz, 2H), 3.18 (d, $J = 6.8$ Hz, 2H), 1.96-1.86 (m, 1H), 1.78 (dd, $J = 12.8$ Hz, 1.6 Hz, 2H), 1.44-1.38 (m, 2H); LC/MS (ESI, m/z) 293.96 $[\text{M}+\text{H}]^+$.

4.1.30. Compound **62** was prepared following the synthetic procedure of **61**.

4-Bromo-2-((tetrahydro-2H-pyran-4-yl)methoxy)thiazole (62) Yield = 73%. ^1H NMR (400 MHz, CDCl_3) δ 6.58 (s, 1H), 4.28 (d, 2H), 3.99-4.02 (m, 4H), 3.39-3.46 (m, 2H), 2.02-2.15 (m, 1H), 1.42-1.72 (m, 2H); LC/MS (ESI, m/z) 277.99 $[\text{M}+\text{H}]^+$.

4.1.31.

4-(5-Chloro-2-fluoropyridin-4-yl)-2-(((tetrahydro-2H-pyran-4-yl)methyl)thio)thiazole (63) A mixture of **61** (2.0 g, 7.22 mmol), **45a** (3.71 g, 14.41 mmol), $\text{Pd}(\text{PPh}_3)_4$ (0.16 g, 0.22 mmol) and Na_2CO_3 (2.35 g, 21.66 mmol) in 1,4-dioxane (20 mL) and H_2O (4 mL) was exchanged with N_2 for three times and the reaction mixture was stirred at 90°C overnight. The resulting mixture was cooled to room temperature and H_2O (80 mL) was added. The aqueous phase was extracted with ethyl acetate (3×30 mL) and the combined organic layers were dried over anhydrous Na_2SO_4 and then concentrated under reduced pressure. The residue was purified by silica gel flash chromatography (eluting with ethyl acetate in petroleum ether 3%) to afford **63** as an off-white solid (0.27 g, yield = 61%); LC/MS (ESI, m/z) 345.03 $[\text{M}+\text{H}]^+$.

4.1.32. Compound **64** was prepared following the synthetic procedure of **63**.

4-(5-Chloro-2-fluoropyridin-4-yl)-2-((tetrahydro-2H-pyran-4-yl)methoxy)thiazole (**64**)

Yield = 42%. ¹H NMR (400 MHz, CDCl₃) δ 8.24 (s, 1H), 7.73 (s, 1H), 7.64 (d, *J* = 1.6 Hz, 1H), 4.35 (d, *J* = 6.8 Hz, 2H), 4.04 (dd, *J* = 11.2 Hz, 4.0 Hz, 2H), 3.45 (td, *J* = 12.0 Hz, 2.0 Hz, 2H), 2.16-2.13 (m, 1H), 1.75 (dd, *J* = 12.8 Hz, 2.0 Hz, 2H), 1.49 (qd, *J* = 12.5 Hz, 4.4 Hz, 2H); LC/MS (ESI, *m/z*) 329.05 [M+H]⁺.

4.1.33. Compound **65** was prepared following the synthetic procedure of **52a**.

tert-butyl (4-bromothiazol-2-yl)((tetrahydro-2H-pyran-4-yl)methyl)carbamate (**65**) Yield = 88%. ¹H NMR (400 MHz, CDCl₃) δ 6.87 (s, 1H), 4.80-4.84 (m, 2H), 1.58 (s, 9H); LC/MS (ESI, *m/z*) 304.98 [M+H-56]⁺.

4.1.34.

(2-((tert-Butoxycarbonyl)((tetrahydro-2H-pyran-4-yl)methyl)amino)thiazol-4-yl)boronic acid (**66**) A mixture of **65** (1.0 g, 12.9 mmol), Bis(pinacolato)diboron (1.0 g, 3.98 mmol) and KOAc (0.52 g, 5.3 mmol) in dioxane (20 mL) was exchanged with argon twice, then Pd(dppf)Cl₂·DCM (0.22 g, 0.26 mmol) were added to the above mixture. The reaction mixture was heated to 100 °C and stirred for 3 h under argon atmosphere. The mixture was concentrated and the residue was purified by silica gel flash chromatography (eluting with ethyl acetate in petroleum ether 5-100%) to give the product **65** as a brown solid (3.2 g, yield = 55%). LC/MS (ESI, *m/z*) 343.15 [M+H]⁺.

4.1.35.

tert-butyl

(4-(2-Chloro-5-methylpyridin-4-yl)thiazol-2-yl)((tetrahydro-2H-pyran-4-yl)methyl)carbamate (**67**) A mixture of **66** (0.35 g, 1.02 mmol), 4-bromo-2-chloro-5-methylpyridine (0.32 g, 1.53 mmol) and K₃PO₄ (0.43 g, 2.04 mmol) in dioxane (15 mL) was exchanged

with argon twice, then PdPPh₃)₄ (0.11 g, 0.1 mmol) were added to the above mixture. The reaction mixture was heated to 100 °C and stirred for 4 h under argon atmosphere. The mixture was concentrated and the residue was purified by silica gel flash chromatography (eluting with ethyl acetate in petroleum ether 5%) to give the product **67** as a white solid (0.3 g, yield = 69%). ¹H NMR (400 MHz, CDCl₃) δ 8.25 (s, 1H), 7.64 (m, 2H), 7.19 (s, 1H), 4.07 (d, *J* = 7.0 Hz, 2H), 3.99 (dd, *J* = 11.3, 3.2 Hz, 2H), 3.35 (td, *J* = 11.8, 2.1 Hz, 2H), 2.49 (s, 3H), 2.22-2.16 (m, 1H), 1.60 (s, 9H), 1.50-1.42 (m, 3H). LC/MS (ESI, *m/z*) 424.14 [M+H]⁺.

4.1.36.

tert-Butyl

(4-(2-(((1*r*,4*r*)-4-((*tert*-butoxycarbonyl)amino)cyclohexyl)amino)-5-methylpyridin-4-yl)thiazol-2-yl)((tetrahydro-2*H*-pyran-4-yl)methyl)carbamate (**68**) A mixture of **67** (0.3 g, 0.71 mmol), *tert*-butyl ((1*r*,4*r*)-4-aminocyclohexyl)carbamate (0.18 g, 0.85 mmol), Binap (0.09 g, 0.14 mmol) and *t*BuONa (0.27 g, 2.84 mmol) in toluene (20 mL) was exchanged with argon twice, then Pd₂(dba)₃ (0.064 g, 0.07 mmol) were added to the above mixture. The reaction mixture was heated to 120 °C overnight under argon atmosphere. The mixture was concentrated and the residue was purified by silica gel flash chromatography (eluting with ethyl acetate in petroleum ether 30%) to give the product **68** as a yellow solid (0.15 g, yield = 35%). ¹H NMR (500 MHz, CDCl₃) δ 7.94 (s, 1H), 7.07 (m, 2H), 6.72 (s, 1H), 4.07 (d, *J* = 7.1 Hz, 2H), 4.01-3.97 (m, 2H), 3.57 (s, 1H), 3.47 (s, 1H), 3.35 (td, *J* = 11.7, 2.1 Hz, 2H), 2.33 (s, 3H), 2.20-2.14 (m, 3H), 2.07-2.04 (m, 1H), 1.62-1.60 (m, 11H), 1.51-1.42 (m, 11H), 1.31-1.24 (m, 4H). LC/MS (ESI, *m/z*) 602.33 [M+H]⁺.

4.1.37.

(1*r*,4*r*)-*N*1-(5-Methyl-4-(2-(((tetrahydro-2*H*-pyran-4-yl)methyl)amino)thiazol-4-yl)pyridi

n-2-yl)cyclohexane-1,4-diamine (**69**) To a solution of **68** (0.15 g, 0.25 mmol) in DCM (1 mL) was added TFA (1 mL) dropwise. After 1 h until the reaction was complete, the mixture was evaporated to dryness and the crude product was purified by silica gel flash chromatography (eluting with MeOH in DCM 9%) to give the title compound **69** as a yellow oil (66 mg, yield = 66%). ¹H NMR (500 MHz, CD₃OD) δ 7.76 (s, 1H), 6.76 (s, 1H), 6.66 (s, 1H), 3.96-3.92 (m, 2H), 3.62-3.56 (m, 1H), 3.39 (td, *J* = 11.8, 2.1 Hz, 2H), 3.32-3.30 (m, 1H), 3.23 (d, *J* = 6.9 Hz, 2H), 2.89-2.82 (m, 1H), 2.24 (s, 1H), 2.12-2.07 (m, 2H), 2.01-1.90 (m, 3H), 1.72-1.68 (m, 2H), 1.46-1.23 (m, 7H). ¹³C NMR (125 MHz, CD₃OD) 169.5, 157.1, 148.7, 147.2, 144.3, 118.7, 108.5, 104.9, 67.3, 50.4, 49.6, 48.9, 34.8, 31.9, 31.0, 30.5, 16.1. LC/MS (ESI, *m/z*) 402.23 [M+H]⁺.

4.2. Biology

4.2.1. *Antibodies and Chemicals.* Phospho-CDK9 (Thr186) antibody (no. 2549S), CDK9 (C12F7) Rabbit mAb (no.2316S), MCL-1 antibody (no. 4572s), BCL-2 (no. 2876s), c-MYC (no. D84C12) XP rabbit mAb (no. 5605) and XIAP antibody (no. 2042) were purchased from Cell Signaling Technology (Danvers, MA). GAPDH (D16H11) XP rabbit mAb (no. HC301) was purchased from TransGen Biotech. Anti-RNA polymerase II CTD repeat YSPTSPS (phospho S5) antibody-ChIP grade (no. ab5131), anti-RNA polymerase II CTD repeat YSPTSPS (phospho S2) antibody-ChIP grade (no. ab5095) were purchased from Abcam. RNA pol II antibody (mAb) (no. 39097) was purchased from Active Motif. Antibodies were used at 1:1000. Cells were lysed for 30 min in lysis buffer supplemented with protease/phosphatase inhibitor cocktail (Cell Signaling Technology). Lysates were cleared by centrifugation at 13 000g at 4 °C for 10 min, and protein concentrations were determined by BCA. Lysates were subjected to

electrophoresis through 10% or 15% gel and immobilized on the nitrocellulose membranes. Compound **7** were purchased from Shanghai MedChem Express (MCE, Shanghai, China).

4.2.2. *Kinase Biochemical Assay.* The ADP-Glo kinase assay (Promega, Madison, WI) was used to screen compounds **11-43** for the CDK9 inhibition potency. The kinase reaction system contains 4.5 μL of CDK9/CyclinK kinase (3 $\text{ng}/\mu\text{L}$), 0.5 μL of serially diluted compounds **11-43**, and 5 μL of CDK9 substrate PDKtide (0.2 $\mu\text{g}/\mu\text{L}$) (Promega, Madison, WI) with 10 μM ATP (Promega, Madison, WI). The reaction in each tube was started immediately by adding ATP and kept going for an hour under 37 $^{\circ}\text{C}$. After the tube was cooled for 5 min at room temperature, 5 μL solvent reactions were carried out in a 384-well plate. Then 5 μL of ADP-Glo reagent was added into each well to stop the reaction and consume the remaining ADP within 40 min. At the end, 10 μL of kinase detection reagent was added into the well and incubated for 30 min to produce a luminescence signal. Luminescence signal was measured with an automated plate reader (Envision, PE, USA) and the dose–response curve was fitted using Prism 7.0 (GraphPad Software Inc., San Diego, CA). The biochemical tests of other targets were provided by Invitrogen (Carlsbad, CA, USA).

4.2.3. *Cell Lines and Cell Culture.* The A375 (melanoma), A431 (squamous), BE(2)M17 (neuroblastoma), BE(2)M17 (neuroblastoma), CRL-2234 (hepatoma), COLO205 (colon cancer), A549 (lung adenocarcinoma), Ramos (B cell lymphoma), MV4-11 (AML), Ramos (B cell lymphoma), U937 (AML), CHL (hamster lung cell), and CHO (hamster ovary cell) cell lines were obtained from American Type Culture Collection (Manassas, VA). OCI-AML-3 (AML), SKM-1 (AML), MEC-1 (CLL),

MEC-2 (CLL) and HL-60 (human promyelocytic leukemia cells) were purchased from Cobioer Biosciences CO., Ltd. (Nanjing, China). Human GIST-T1 cells were kindly provided by the group of professor Jonathan A. Fletcher, Brigham and Women's hospital in Boston, USA. MOLM-13 and MOLM14 cell lines were provided by Dr. Scott Armstrong, Dana Farber Cancer Institute (DFCI), Boston, MA. All the cells were grown in a humidified incubator (Thermo, USA) at 37 °C under 5% CO₂. A375, A431, GIST-T1, A549, Colo205 and CHO cells were maintained in DMEM supplemented with 10% FBS, 1% penicillin/streptomycin. BE(2)M17 cells were cultured with 1:1 mixture of ATCC-formulated Eagle's minimum essential medium, catalog no. 30-2003 and F12 Medium. MV4-11, MEC-1 and MEC-2 were grown in IMDM supplemented with 10% FBS, 1% penicillin/streptomycin. CRL-2234, U2932, U937, Ramos, MOLM13, MOLM14, OCI-AML-3, SKM-1, HL-60 and CHL were grown in Roswell Park Memorial Institute (RPMI) 1640 medium supported with 10% FBS and 1% penicillin/streptomycin. Adherent cells were grown in tissue culture flasks until they were 85–95% confluent prior to use. For suspension cells, cells were collected by spin down at 800 rpm/min for 5 min before use.

Cells were grown in 96-well culture plates (3000 cells/well). The compounds at various concentrations were added into the plates. Cell proliferation was determined after treatment with compounds for 72 h. Cell viability was measured using the Cell Titer-Glo assay (Promega, USA) according to the manufacturer's instructions and luminescence was measured in a multilabel reader (Envision, PerkinElmer, USA). Data were normalized to control groups (DMSO) and represented by the mean of three independent

measurements with standard error of <20%. GI₅₀ values were calculated using Prism 7.0 (GraphPad Software, San Diego, CA).

4.2.4. *Signaling Pathway Study.* MV4-11, HL-60 and MEC-1 cells were treated with DMSO, serially diluted compound **40**, 1 μ M compound **7** for 2 h. Cells were then washed in 1 \times PBS and lysed in cell lysis buffer. Phospho-CDK9 (Thr186), CDK9, Phospho-RNA Pol II (Ser2), Phospho-RNA Pol II (Ser5), RNA Pol II, XIAP, MCL-1, C-MYC, BCL-2 and GAPDH antibody (Cell Signaling Technology) were used for immunoblotting.

4.2.5. *Apoptosis Effect Examination.* MV4-11, HL-60 and MEC-1 cells were treated with DMSO, serially diluted compound **40**, 0.01 μ M compound **7** for indicated periods. Cells were then washed in PBS and lysed in cell lysis buffer. PARP, caspase-3, GAPDH antibody (Cell Signaling Technology) were used for immunoblotting.

4.2.6. *Cell Cycle Analysis.* MV4-11, HL-60 and MEC-1 cells were treated with DMSO, serially diluted compound **40**, 0.01 or 0.1 μ M compound **7** for indicated periods. The cells were fixed in 70% cold ethanol and incubated at -20 °C overnight and then stained with PI/RNase staining buffer (BD Pharmingen). Flow cytometry was performed using a FACS Calibur (BD) and the results were analyzed by ModFit software.

4.2.7. *Modeling Method.* All simulations were performed using Schrödinger Suites 2017. Preparation of the crystal structures of CDK7/CDK9 were carried out with the Protein Preparation Wizard module. A restrained partial minimization was then performed with the maximum root-mean-square deviation (RMSD) value set to 0.18 Å. Preparation of the ligands were all accomplished by the LigPrep module with protonated states generated at pH = 7.0 \pm 2.0. All other parameters were set to the default values.

Compounds **9** and **40** were docked into the binding pocket of CDK7/9 using the extended sampling protocol of IFD.

4.2.8. *Pharmacokinetics Study.* This study protocol was approved by the animal ethics committee of Hefei Institutes of Physical Science, Chinese Academy of Sciences (Hefei, China). The male Sprague–Dawley rats (190-210 g) were provided by laboratory animal center of Anhui Medical University (Hefei, China). The animals were housed in an air-conditioned animal room at a temperature of 23 ± 2 °C and a relative humidity of $50 \pm 10\%$ and allowed free access to tap water and lab. The mice, rats and dogs were acclimatized to the facilities for one week and then fasted for 12 h with free access to water prior to the experiment. The mice (48), rats (6) or dogs (6) were randomly and equally divided into two groups for the compound's pharmacokinetic study. One group was injected with *i.v.* formulation at a dose of 3 mg/kg, 3 mg/kg and 2 mg/kg in mice, rats and dogs respectively. The other group was treated by oral administration of *p.o.* formulation at doses of 10 mg/kg, 20 mg/kg and 10 mg/kg in mice, rats and dogs respectively. The *p.o.* formulation of compound **40** for mice and dogs was consisted of 10 mg compound **40** dissolved in 0.5 mL of dimethyl sulfoxide and 4.5 mL of 5% glucose water, and the *p.o.* formulation for rats was made with 20 mg compound **40** dissolved in 1 mL of dimethyl sulfoxide and 4 mL of 5% glucose water. The *i.v.* formulation of compound **40** is made with 0.5 mL of the *p.o.* formulation and 4.5 mL of 5% glucose water. About 300 μ L of blood samples were collected into heparinized tubes at 2, 5, 15, 30, 60, 120, 240, 360, 540 and 720 min after intravenous injection and at 5, 15, 30, 60, 90, 120, 240, 360, 540 and 720 min after oral administration. 100 μ L of plasma was harvested by centrifuging the blood sample at 4 °C and 5000 rpm for 3 min, and then

stored at $-80\text{ }^{\circ}\text{C}$ until analysis. An aliquot of $100\text{ }\mu\text{L}$ of each plasma sample was mixed with $20\text{ }\mu\text{L}$ of internal standard working solution (200 ng/mL of caffeine). Methanol ($400\text{ }\mu\text{L}$) was then added for precipitation. After vortexing for 5 min and centrifuging at $14,000\text{ rpm}$ for 10 min , $5\text{ }\mu\text{L}$ of the supernatant was injected for LC-MS/MS analysis. The pharmacokinetic parameters were analyzed through noncompartment model using WinNonlin 6.1 software (Pharsight Corporation, Mountain View, USA), including half-life ($T_{1/2}$), plasma concentration at 0 min (C_0), the peak of the plasma concentration (C_{max}), the time to peak of the plasma concentration (T_{max}), the area under the plasma concentration-time curve during the period of observation (AUC_{0-t}), the area under the plasma concentration-time curve from zero to infinity ($\text{AUC}_{0-\infty}$), clearance (Cl), apparent volume of distribution (Vd) and the mean residence time (MRT). The oral bioavailability (F) is calculated according to the following equation: $F = \text{AUC}_{0-\infty}(\text{oral}) / \text{AUC}_{0-\infty}(\text{iv}) \times \text{dose}(\text{iv}) / \text{dose}(\text{oral}) \times 100\%$.

4.2.9. *MV4-11 Xenograft Tumor Model.* Five-week-old female nu/nu mice were purchased from the Shanghai experimental center, Chinese Academy of Sciences (Shanghai, China). All animals were housed in a specific pathogen-free facility and used according to the animal care regulations of Hefei Institutes of Physical Science, Chinese Academy of Sciences (Hefei, China). Prior to implantation, cells were harvested during exponential growth. Five million MV4-11 cells in PBS were formulated as a 1:1 mixture with Matrigel (BD Biosciences) and injected into the subcutaneous space on the right flank of nu/nu mice. Daily oral administration was initiated when MV4-11 tumors had reached a size of $200\text{--}400\text{ mm}^3$. Animals were then randomized into treatment groups of 5 mice each for efficacy studies. Compound **40** was delivered daily in a HKI solution

(0.5% methocellulose/0.4% Tween80 in *ddH*₂O) by oral gavage. A range of doses of **40** or its vehicle as control were administered. Body weight was measured daily and tumor growth was measured every day after **40** treatment. Tumor volume was calculated as follows: tumor volume (mm³) = [(W² × L)/2] in which width (W) is defined as the smaller of the two measurements and length (L) is defined as the larger of the two measurements. Animal experiments were performed after approval and in accordance with the guidelines of the Animal Care and Use Committee at the High Magnetic Field Laboratory, Chinese Academy of Sciences, P. R. China.

4.2.10. *Statistical analysis.* The experimental results were quantified by GraphPad Prism 7 (Version 7.0, GraphPad Software, La Jolla, CA). Comparisons between treatments were analyzed by Student's t test. P values were labelled in figures and Standard Deviations are shown.

Author contributions

The manuscript was written through contributions of all authors. All authors have given approval to the final version of the manuscript.

Acknowledgments

This work was supported by the National Natural Science Foundation of China (Grants U1432250, 81471773, 81473088, U1532154, 81703559, 81703007, 21708044), the National Key Research and Development Program of China (Grant 2016YFA0400900), the Major Science and Technology Program of Anhui Province (Grant 16030801114), the China Postdoctoral Science Foundation (Grants 2018M630721, 2018T110633, 2018T110634), the Natural Science Foundation of Anhui Province

(Grants 1808085MH268, 1708085MH208, 1808085MH274, 1808085QH263) and the Frontier Science Key Research Program of CAS (Grant QYZDB-SSW-SLH037). We are also grateful for the National Program for Support of Top-Notch Young Professionals for J.L.

Appendix A. Supplementary data

Supplementary data related to this article can be found at XXXXXX.

References

- [1] T. Hunter, J. Pines, Cyclins and Cancer II: Cyclin D and CDK Inhibitors Come of Age. *Cell* 79 (1994) 573–582.
- [2] C.J. Sherr, Cancer Cell Cycles. *Science* 274 (1996) 1672–1677.
- [3] H. Matsushime, D.E. Quelle, S.A. Shurtleff, M. Shibuya, C.J. Sherr, J.Y. Kato, D-Type Cyclin-Dependent Kinase Activity in Mammalian Cells. *Mol. Cell Biol.* 14 (1994) 2066–2076.
- [4] U. Asghar, A. K. Witkiewicz, N.C. Turner, E.S. Knudsen, The History and Future of Targeting Cyclin-Dependent Kinases in Cancer Therapy. *Nat. Rev. Drug Discov.* 14 (2015) 130–146.
- [5] S. Lapenna, A. Giordano, Cell Cycle Kinases as Therapeutic Targets for Cancer. *Nat. Rev. Drug Discov.* 8 (2009) 547–566.
- [6] M. Tutone, A. M. Almerico, Recent advances on CDK inhibitors: An insight by means of in silico methods. *Eur. J. Med. Chem.* 142 (2017) 300-315.
- [7] S. Kalra, G. Joshi, A. Munshi, R. Kumar, Structural insights of cyclin dependent kinases: Implications in design of selective inhibitors. *Eur. J. Med. Chem.* 142 (2017) 424-458.

- [8] S. Wang, P.M. Fischer, Cyclin-Dependent Kinase 9: A Key Transcriptional Regulator and Potential Drug Target in Oncology, Virology and Cardiology. *Trends Pharmacol. Sci.* 29 (2008) 302–313.
- [9] R.J. Sims, R. Belotserkovskaya, D. Reinberg, Elongation by RNA Polymerase II: The Short and Long of It. *Genes. Dev.* 18 (2004) 2437–2468.
- [10] G. Napolitano, P. Licciardo, A.L.L. Giordano, B. Majello, Transcriptional Activity of P-TEF β Kinase in Vivo Requires the C-Terminal Domain of RNA Polymerase II. *Gene* 254 (2000) 139–145.
- [11] K. Bettayeb, D. Baunbæk, C. Delehouze, N. Loaëc, A.J. Hole, S. Baumli, J.A. Endicott, S. Doucrazy, J. Bénard, N. Oumata, CDK Inhibitors Roscovitine and CR8 Trigger Mcl-1 Down-Regulation and Apoptotic Cell Death in Neuroblastoma Cells. *Genes & Cancer* 1 (2010) 369–380.
- [12] Y.A. Sonawane, M.A. Taylor, J.V. Napoleon, S. Rana, J.I. Contreras, A. Natarajan, Cyclin Dependent Kinase 9 Inhibitors for Cancer Therapy. *J. Med. Chem.* 59 (2016) 8667–8684.
- [13] E. Walsby, G. Pratt, H. Shao, A.Y. Abbas, P.M. Fischer, T.D. Bradshaw, P. Brennan, C. Fegan, S. Wang, C. Pepper, A Novel CDK9 Inhibitor Preferentially Targets Tumor Cells and Synergizes with Fludarabine. *Oncotarget* 5 (2014) 375–385.
- [14] S. Wang, G. Griffiths, C.A. Midgley, A.L. Barnett, M. Cooper, J. Grabarek, L. Ingram, W. Jackson, G. Kontopidis, S.J. McClue, C. McInnes, J. McLachlan, C. Meades, M. Mezna, I. Stuart, M. P. Thomas, D.I. Zheleva, D.P. Lane, R.C. Jackson, D.M. Glover, D.G. Blake, P.M. Fischer, Discovery and Characterization of

2-Anilino-4-(Thiazol-5-yl)Pyrimidine Transcriptional CDK Inhibitors as Anticancer Agents, *Chem. Biol.* 17 (2010) 1111–1121.

[15] R. Chen, M. J. Keating, V. Gandhi, W. Plunkett, Transcription Inhibition by Flavopiridol: Mechanism of Chronic Lymphocytic Leukemia Cell Death *Blood* 106 (2005) 2513–2519.

[16] K. Vladimir, B. Sonja, F. Robert, Perspective of Cyclin-Dependent Kinase 9 (CDK9) as a Drug Target. *Curr. Pharm. Design* 18 (2012) 2883–2890.

[17] R.N. Misra, H.Y. Xiao, K.S. Kim, S. Lu, W.C. Han, S.A. Barbosa, J.T. Hunt, D.B. Rawlins, W. Shan, S.Z. Ahmed, L. Qian, B.C. Chen, R. Zhao, M.S. Bednarz, K.A. Kellar, J.G. Mulheron, R. Batorsky, U. Roongta, A. Kamath, P. Marathe, S.A. Ranadive, J.S. Sack, J.S. Tokarski, N.P. Pavletich, F.Y F. Lee, K.R. Webster, S.D. Kimball, N-(Cycloalkylamino)Acyl-2-Aminothiazole Inhibitors of Cyclin-Dependent Kinase 2. N-[5-[[[5-(1,1-Dimethylethyl)-2-Oxazolyl]Methyl]Thio]-2-Thiazolyl]-4-Piperidinecarboxamide (BMS-387032), a Highly Efficacious and Selective Antitumor Agent. *J. Med. Chem.* 47 (2004) 1719–1728.

[18] A. Conroy, D. EStockett, DWalker, M. RArkin, U. Hoch, J.A. Fox, R.E. Hawtin, SNS-032 Is a Potent and Selective CDK 2, 7 and 9 Inhibitor That Drives Target Modulation in Patient Samples. *Cancer Chemother Pharmacol* 64 (2009) 723–732.

[19] D. Cirstea, T. Hideshima, S. Pozzi, S. Vallet, H. Ikeda, L. Santo, H. Loferer, N. Vaghela, Y. Okawa, G. Perrone, G. Gorgun, E. Calabrese, N.C. Munshi, Anderson, K. C.; Raje, N. RGB 286638, a Novel Multi-Targeted Small Molecule Inhibitor, Induces Multiple Myeloma (MM) Cell Death through Abrogation of CDK-dependent and -Independent Survival Mechanisms. *Blood* 112 (2008) 2759–2759.

- [20] D. Cirstea, T. Hideshima, L. Santo, H. Eda, Y. Mishima, N. Nemani, Y. Hu, N. Mimura, F. Cottini, G. Gorgun, H. Ohguchi, R. Suzuki, H. Loferer, N.C. Munshi, K.C. Anderson, N. Raje, Small-Molecule Multi-Targeted Kinase Inhibitor RGB-286638 Triggers P53-Dependent and -Independent Anti-Multiple Myeloma Activity through Inhibition of Transcriptional CDKs. *Leukemia* 27 (2013) 2366–2375.
- [21] K.F. Byth, A. Thomas, G. Hughes, C. Forder, A. McGregor, C. Geh, S. Oakes, C. Green, M. Walker, N. Newcombe, S. Green, J. Growcott, A. Barker, R.W. Wilkinson, AZD5438, a Potent Oral Inhibitor of Cyclin-Dependent Kinases 1, 2, and 9, Leads to Pharmacodynamic Changes and Potent Antitumor Effects in Human Tumor Xenografts. *Mol. Cancer Ther.* 8 (2009) 1856–1866.
- [22] M.S. Squires, R.E. Feltell, N.G. Wallis, E.J. Lewis, D.M. Smith, D.M. Cross, J. F. Lyons, N.T. Thompson, Biological Characterization of AT7519, a Small-Molecule Inhibitor of Cyclin-Dependent Kinases, in Human Tumor Cell Lines. *Mol. Cancer Ther.* 8 (2009) 324–332.
- [23] J. Flynn, J. Jones, A.J. Johnson, L. Andritsos, K. Maddocks, S. Jaglowski, J. Hessler, M.R. Grever, E. Im, H. Zhou, Y. Zhu, D. Zhang, K. Small, R. Bannerji, J.C. Byrd, Dinaciclib Is a Novel Cyclin-Dependent Kinase Inhibitor with Significant Clinical Activity in Relapsed and Refractory Chronic Lymphocytic Leukemia. *Leukemia* 29 (2015) 1524–1529.
- [24] D. Parry, T. Guzi, S F. hanahan, N. Davis, D. Prabhavalkar, D. Wiswell, W. Seghezzi, K. Paruch, M.P. Dwyer, R. Doll, A. Nomeir, W. Windsor, T. Fischmann, Y. Wang, M. Oft, T. Chen, P. Kirschmeier, E.M. Lees, Dinaciclib (SCH 727965), a Novel and Potent Cyclin-Dependent Kinase Inhibitor. *Mol. Cancer Ther.* 9 (2010) 2344–2353.

- [25] K. Paruch, M. P. Dwyer, C. Alvarez, C. Brown, T.Y. Chan, R.J. Doll, K. Keertikar, C. Knutson, B. Mckittrick, J. Rivera, Discovery of Dinaciclib (SCH 727965): A Potent and Selective Inhibitor of Cyclin-Dependent Kinases. *ACS Med. Chem. Lett.* 1 (2010) 204–208.
- [26] C.M. Olson, B. Jiang, M.A. Erb, Y. Liang, Z.M. Doctor, Z. Zhang, T. Zhang, N. Kwiatkowski, M. Boukhali, J.L. Green, W. Haas, T. Nomanbhoy, E.S. Fischer, R.A. Young, J. E. Bradner, G.E. Winter, N.S. Gray, Pharmacological Perturbation of CDK9 Using Selective CDK9 Inhibition or Degradation. *Nat. Chem. Biol.* 14 (2017) 163–170.
- [27] H. Shao, S. Shi, S. Huang, A.J. Hole, A.Y. Abbas, S. Baumli, X. Liu, F. Lam, D.W. Foley, P.M. Fischer, M. Noble, J.A. Endicott, C. Pepper, S. Wang, Substituted 4-(Thiazol-5-yl)-2-(Phenylamino)Pyrimidines Are Highly Active CDK9 Inhibitors: Synthesis, X-Ray Crystal Structures, Structure–Activity Relationship, and Anticancer Activities. *J. Med. Chem.* 56 (2013) 640–659.
- [28] R. Wilcken, M.O. Zimmermann, A. Lange, A.C. Joerger, F.M. Boeckler, Principles and Applications of Halogen Bonding in Medicinal Chemistry and Chemical Biology. *J. Med. Chem.* 56 (2013) 1363–1388.
- [29] K. Saotome, H. Morita, M. Umeda, Cytotoxicity Test with Simplified Crystal Violet Staining Method Using Microtitre Plates and Its Application to Injection Drugs. *Toxicol. In Vitro.* 3 (1989) 317–321.
- [30] M.A. Fabian, W.H. Biggs III, D.K. Treiber, C.E. Atteridge, M.D. Azimioara, M.G. Benedetti, T.A. Carter, P. Ciceri, P.T. Edeen, M. Floyd, J.M. Ford, M. Galvin, J.L. Gerlach, R.M. Grotzfeld, S. Herrgard, D.E. Insko, M.A. Insko, A.G. Lai, J.M. Lélías, S. A. Mehta, Z.V. Milanov, A.M. Velasco, L.M. Wodicka, H.K. Patel, P.P. Zarrinkar, D.J.

Lockhart, A Small Molecule–Kinase Interaction Map for Clinical Kinase Inhibitors. *Nat. Biotechnol.* 23 (2005) 329–336.

[31] G. Polier, J. Ding, B. V. Konkimalla, D. Eick, N. Ribeiro, R. Köhler, M. Giasi, T. Efferth, L. Desaubry, P.H. Kramer, Wogonin and Related Natural Flavones Are Inhibitors of CDK9 That Induce Apoptosis in Cancer Cells by Transcriptional Suppression of Mcl-1. *Cell Death Dis.* 2 (2011) e182.

Highlights

- Highly potent CDK9 inhibitor **40** ($IC_{50} = 1$ nM)
- Achieved 300-10000 fold selectivity over other CDK kinase family members
- High selectivity over other 468 kinases/mutants (KINOMEscan S score(1)=0.01)
- Potently inhibited the phosphorylation of RNA Pol II Ser2 (EC_{50} : <100 nM)